NASA TN D-1570

74p.

TECHNICAL NOTE

D-1570

ORBIT-LAUNCHED NUCLEAR VEHICLE DESIGN AND PERFORMANCE EVALUATION PROCEDURE FOR ESCAPE AND PLANETARY MISSIONS

By Ronald J. Harris and Robert E. Austin

George C. Marshall Space Flight Center
Huntsville, Alabama

NATIONAL AERONAUTICS AND SPACE ADMINISTRATION
WASHINGTON
June 1963

Table-1

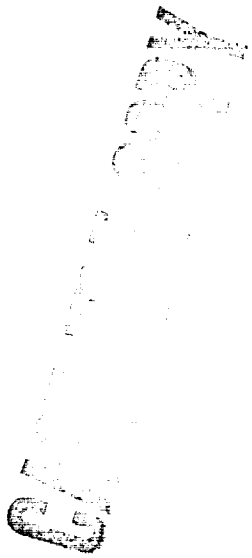

TABLE OF CONTENTS

LIST OF ILLUSTRATIONS

LIST OF ILLUSTRATIONS (Cont'd)

LIST OF ILLUSTRATIONS (Cont'd)

LIST OF TABLES

DEFINITION OF SYMBOLS

Symbol	Definition
A	Specific weight parameter proportional to thrust
B	Specific weight parameter proportional to propellant loading
C	Specific weight parameter proportional to initial gross weight in orbit
F	Thrust
F/W_o	Initial thrust-to-weight ratio based on sea level weight, or initial acceleration measured in multiples of g_n
f_e	Hyperbolic excess fraction; $\frac{V_\infty}{V_\oplus}$
g	Acceleration of gravity
g_n	Mean apparent gravity at sea level; international standard for weight-mass conversion; 9.81992 m/sec^2
h	Altitude, $r - r_\oplus$
h_b	Burnout altitude, $r_b - r_\oplus$
h_o	Altitude of initial orbit, $r_o - r_\oplus$
I_{sp}	Specific impulse
m	Mass
r	Radius from center of earth to vehicle
r_o	Radius of initial orbit
$r_\oplus$	Radius of mean spherical earth
t	Flight time
V	Inertial velocity

DEFINITION OF SYMBOLS (Cont'd)

Symbol	Definition
V_e	Escape velocity
ΔV_{id}	Characteristic velocity
V_p	Injection velocity
$V_\oplus$	Earth's mean orbital velocity
V_∞	Hyperbolic excess velocity
W_o	Initial weight in orbit
W_n	Effective net structural weight
W_{gd}	Gross payload weight
W_s	Useable propellant weight
β	Thrust vector orientation angle measured from the velocity vector to the thrust vector (positive down)
θ	Flight path angle, measured from the local vertical (positive down)
ψ	Central angle measured from local radius vector at ignition
ζ	Propellant ratio, $\frac{W_s}{W_o}$
λ_{gd}	Gross payload ratio, $\frac{W_{gd}}{W_o}$
$\mu_\oplus$	Gravitational constant of earth

Subscripts

o	Initial
$\oplus$	Earth

DEFINITION OF SYMBOLS (Concluded)

Subscripts	Definition
ref	Denotes reference conditions
100	Denotes a change in a parameter due to a 100 N. M. change in h_o
A, B, h_o, I_{sp}	Indicate that a parameter is calculated for arbitrary values of A, B, h_o or I_{sp} respectively

Abbreviations	
deg	Degrees
km	Kilometers
m	Meters
lb	Pounds
N. M.	Nautical miles
sec	Seconds
Wt	Weight

NATIONAL AERONAUTICS AND SPACE ADMINISTRATION

TECHNICAL NOTE D-1570

ORBIT-LAUNCHED NUCLEAR VEHICLE DESIGN AND PERFORMANCE EVALUATION PROCEDURE FOR ESCAPE AND PLANETARY MISSIONS

By

Ronald J. Harris and Robert E. Austin

SUMMARY

A comprehensive procedure is described, and reference data presented, by which the effect of certain design parameters upon the basic performance of orbit-launched nuclear vehicles can be readily determined for escape and planetary missions. The performance parameters investigated are payload ratio, propellant ratio, characteristic velocity requirement, burning time, injection altitude, central angle and flight path angle. The effects of initial thrust-to-weight ratio, initial altitude, specific impulse, specific weight factors and hyperbolic excess velocity are considered. The range of specific impulse assumed is restricted to that considered practical for nuclear heat exchanger propulsion systems.

Use of this procedure and the data presented allows a quick determination of nuclear propulsion requirements for specific mission profiles from the standpoint of maximizing either payload or payload ratio. It is shown that, in general, maximum payload and maximum payload ratio are not coincident when thrust is fixed and initial weight is variable. It is further shown that, for certain hyperbolic excess velocities, there is an optimum initial weight in orbit when operating with a fixed engine system within the range of thrust-to-weight ratios considered practical for nuclear heat exchanger systems.

Numerical examples are included which illustrate the methodology and indicate the degree of accuracy that can be expected of the estimation procedure. The results of the numerical examples are compared with exact computer solutions and shown to be well within the accuracy usually required in preliminary design studies.

INTRODUCTION

With increasing interest in the consideration of interplanetary travel via nuclear rocket space systems, it becomes important to have available a rapid unsophisticated and practical method for relating nuclear vehicle design and performance parameters to trajectory characteristics once preliminary mission profiles and conceptual vehicles are established. A comprehensive procedure of this nature can provide a useful tool for conducting feasibility studies of contemplated missions. The methodology used must have an inherent accuracy sufficient for preliminary design studies.

The purpose of this report is to present reference data and a procedure by which the effect of certain design parameters upon the basic performance of orbit-launched nuclear vehicles can be determined. Beyond simple space probes, interplanetary missions will require large initial gross weights in orbit. Conventional chemical vehicles are inefficient for such missions and hence the range of specific impulse assumed in this report is restricted to the range considered practical for the more efficient nuclear heat-exchanger propulsion systems, namely 700 to 1000 sec. While the reference data presented is restricted to nuclear rocket systems, the general method of performance estimation can be applied with equivalent success to any orbit-launched system.

The approach used, in establishing a flexible method of mission evaluation, is based on the analysis described in Reference 1. However, Reference 1 is limited to typical lunar and escape missions and is concerned primarily with the influence of structural weight parameters on the optimum thrust-to-weight ratio of orbit-launched vehicles. It is pointed out in Reference 1 that a discussion of payload performance is possible only when representative vehicle structural and engine weight parameters are introduced. This report extends the analysis of Reference 1 to include interplanetary missions requiring hyperbolic excess velocities.

The hyperbolic excess velocity, V_∞, a convenient parameter for describing the energy requirements necessary for interplanetary missions, is the residual velocity of the vehicle with respect to Earth, when the vehicle-earth distance is very large (Ref. 2). Furthermore, if the resulting heliocentric orbital eccentricity is near unity, the hyperbolic excess velocity can also be thought of as the difference between the orbital velocity of the Earth and the perihelion velocity or aphelion velocity of the transfer ellipse to the target planet, depending upon whether the targer planet moves outside or inside respectively, of the earth's orbit (Ref. 3). Hyperbolic excess velocity is commonly quoted as a fraction, f_e, of the earth's mean orbital velocity, a procedure which is adopted in this report. The values of f_e considered range from zero, corresponding to parabolic escape velocity, to 0.5, representing an extremely high energy requirement. This range of hyperbolic excess velocity covers the practical spectrum characteristic of the earth injection phase of missions of Mars and Venus (Ref. 4 and 5).

For escape missions it is shown in Reference 1 that for a given orbit-launched vehicle system, the tangential thrust vector orientation mode is superior to the circumferential control mode. Reference 6 further shows that the tangential mode is near optimum for missions requiring hyperbolic excess velocities. Consequently only tangential thrust is considered in this report, with thrust assumed to be of constant magnitude. A single stage is assumed from earth orbit to final injection. Initial thrust-to-weight ratio, F/W_o, is varied between 0.04 and 0.5, with both limits being selected arbitrarily. The lower limit may not be practical for early generation nuclear systems due to burning time restrictions. Initial orbit altitudes are assumed to lie between 100 N.M. (185.3 km) and 400 N.M. (741.2 km).

The various vehicle and performance parameters considered include payload ratio, propellant ratio, velocity requirement, burning time, injection altitude, central angle and flight path angle. Reference curves are presented for each of these parameters over the range of hyperbolic excess velocities assumed, along with correction curves to allow for variations in specific impulse and initial orbit altitude. Furthermore, it is shown that variations in vehicle structural and engine weights can be accounted for with a single algebraic equation.

Calculations were made by numerical integration on the IBM 7090 digital computer. The equations of motion are related to a spherical Earth. The analysis is limited to planar trajectories with all aerodynamic and pertubative forces being neglected.

Several numerical examples are included which illustrate typical performance estimations. The accuracy obtained is shown to be well within the limits required of preliminary design studies.

ANALYSIS

The method of calculation of the parametric data presented in this report is based primarily on the analysis described in Reference 1. However, since Reference 1 is limited to a consideration of lunar and escape trajectories, it is necessary in the present analysis to express the injection velocity in terms of the hyperbolic excess velocity. Since the thrust is assumed to be purely tangential, no attitude restriction can be placed on the resulting trajectory. Hence, the attainment of the desired velocity is assumed to be sufficient for proper injection.

Referring to Reference 1 and the sketch presented below, the general equations ıotion of a vehicle leaving orbit are:

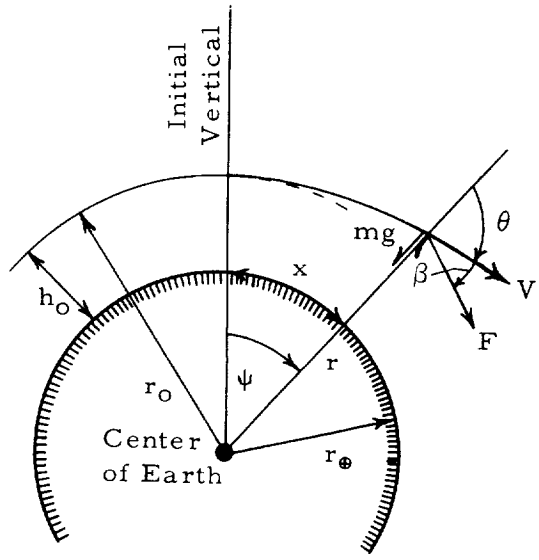

$$\dot{v} = \frac{F \cos \beta}{m} - g \cos \theta$$

$$\dot{\theta} = \frac{F \sin \beta}{mv} + \left(\frac{g}{v} - \frac{v}{r}\right) \sin \theta$$

For the assumption of tangential thrust ($\beta = 0°$), these equations reduce to

$$\dot{v} = \frac{F}{m} - g \cos \theta \qquad (1)$$

$$\dot{\theta} = \left(\frac{g}{v} - \frac{v}{r}\right) \sin \theta \qquad (2)$$

Numerical integration of the equations of motion determines velocity and flight path angle. Thus,

$$v = \int \dot{v}\, dt \tag{3}$$

$$\theta = \int \dot{\theta}\, dt \tag{4}$$

Range and altitude are then calculated by the respective relations

$$x = \int \frac{r_{\oplus}}{r}\, v \sin\theta\, dt \tag{5}$$

$$h = h_o + \int v \cos\theta\, dt \tag{6}$$

The central angle is found from

$$\psi = \int \frac{\dot{x}}{r_{\oplus}}\, dt \tag{7}$$

It should be noted that the initial thrust-to-weight ratio is hidden in equation 1 since,

$$\frac{F}{m} = \left(\frac{F}{W_o}\right) g_n$$

As pointed out in Reference 1, the weight characteristics of the vehicle must be defined before an evaluation of payload performance can be made. The effective net structural weight of a vehicle stage, W_n, is assumed to be composed of three weight groups proportional to the thrust, propellant loading and initial weight of the stage, respectively. The first weight group is composed of the engine, propulsion system hardware, and any structural members which may be assumed proportional to thrust.* The second group consists of propellant tankage and any propellant residuals which may be assumed proportional to the propellant loading. The third weight group, which is assumed to be proportional to the initial weight of the vehicle, is composed of astrionic gear, interstage structure and various miscellaneous equipment. Each of these weight groups can be represented by a nondimensional specific weight factor as follows:

*Items listed here are intended to be typical of nuclear systems; user should employ his own discretion in assigning component weight proportionality.

$$A = \frac{\text{Wt proportional to } F}{F} = \frac{\text{Wt of engine, propulsion hardware, etc.}}{F}$$

$$B = \frac{\text{Wt proportional to } W_8}{W_8} = \frac{\text{Wt of tankage, propellant residuals, etc.}}{W_8}$$

$$C = \frac{\text{Wt proportional to } W_o}{W_o} = \frac{\text{Wt of astrionic gear, interstage structure, etc.}}{W_o}$$

The effective net structural weight of a vehicle stage can then be expressed as

$$W_n = AF + BW_8 + CW_o \tag{8}$$

The relation between payload, propellant loading and effective net structural weight is

$$W_{gd} = W_o - W_8 - W_n$$

or

$$W_{gd} = W_o - AF - (B + 1)\, W_8 - CW_o \tag{9}$$

where W_{gd} is the gross payload.

Equation 9 can be expressed in terms of nondimensional ratios by dividing both sides by W_o with the result,

$$\lambda = 1 - A(F/W_o) - (B + 1)\, \zeta - C \tag{10}$$

where

$$\lambda = \frac{W_{gd}}{W_o}$$

$$\zeta = \frac{W_8}{W_o}$$

The specific weight parameter can be assumed equal to zero without affecting the general shape of the payload ratio curve or the location of the optimum thrust-to-weight ratio corresponding to maximum payload ratio (Ref. 1). Hence equation 10 can be written

$$\lambda = (\lambda)_{C = o} - C \tag{11}$$

All reference curves shown in this report for payload ratio are for C equals zero, so that equation 11 must be applied in any practical application of these curves.

For constant thrust and specific impulse, the propellant ratio is given by

$$\zeta = \left(\frac{F}{W_o}\right)\frac{t_b}{I_{sp}} \tag{12}$$

Once ζ is determined, the characteristic velocity can be found from the well-known relation

$$\Delta V_{id} = g_n I_{sp} \ln \frac{1}{1 - \zeta} \tag{13}$$

For missions requiring hyperbolic excess velocity, the injection velocity, V_p, is related to escape velocity, V_e, by the relation

$$V_p = (V_e^2 + V_\infty^2)^{\frac{1}{2}} \tag{14}$$

where V_∞ is the hyperbolic excess velocity. As mentioned earlier, the hyperbolic excess velocity is commonly expressed as a fraction, f_e, of the earth's mean orbital velocity, $V_\oplus$. Hence,

$$f_e = \frac{V_\infty}{V_\oplus} \tag{15}$$

and equation 14 can be written

$$V_p = [\, V_e^2 + (f_e\ V_\oplus)^2]^{\frac{1}{2}}$$

The injection velocity corresponding to a specified hyperbolic excess requirement is a function of altitude since V_e, the local escape velocity, is inversely proportional to altitude.

If reference values are assumed for specific impulse, initial orbit altitude, and specific weight parameters, the various performance parameters can be calculated, varying initial thrust-to-weight and hyperbolic excess velocity over the respective range of values considered. The reference values assumed are arbitrary but should be reasonable and typical since the reference data forms the basis of further performance estimations. The reference conditions assumed in this report are:

$(I_{sp})_{ref}$ = 800 sec

$(h_o)_{ref}$ = 300 N. M.

A_{ref} = B_{ref} = 0. 1

C_{ref} = 0

Reference curves are shown in Figure 1 through 7 for the various performance parameters. It is obvious that the accuracy of a graphical method of performance estimation is dependent upon the accuracy to which the graphs can be read. For preliminary design purposes, payload and characteristic velocity are perhaps the most important of all the performance parameters. Consequently, the curves of payload ratio and characteristic velocity shown in Figure 1 and 2, respectively, are plotted on a highly expanded scale.

Once reference data are delineated for the individual performance parameters, consideration must be given to variations in vehicle specific weights, specific impulse and initial orbit altitude. The effects of such variations and the means of estimating each of the performance parameters will now be discussed.

Payload Ratio

Of all the performance parameters considered, only λ is affected by changes in A and B. For reference conditions, equation 10 can be written

$$\lambda_{ref} = 1 - A_{ref} (F/W_o) - (B_{ref} + 1) \zeta_{ref} \tag{17}$$

where both λ_{ref} and ζ_{ref} are functions of F/W_o and V_∞, as illustrated in Figure 1 and 3, respectively. Arbitrary values of A and B can be expressed in the form,

$$A = A_{ref} + \Delta A$$
$$= 0.1 + \Delta A \tag{18}$$

$$B = B_{ref} + \Delta B$$
$$= 0.1 + \Delta B \tag{19}$$

Hence, for arbitrary values of A and B, equation 17 becomes

$$(\lambda_{ref})_{A,B} = 1 - A\,(F/W_o) - (B + 1)\,\zeta_{ref}$$

where the terminology is adopted that subscripts outside parentheses, or brackets, enclosing one of the performance parameters indicate variable conditions. Hence $(\lambda_{ref})_{A,B}$ denotes λ at reference conditions with the exception of A and B which are variable. It follows that the change in payload ratio from reference conditions due to a change in A and B is,

$$\Delta\lambda_{A,B} = (\lambda_{ref})_{A,B} - \lambda_{ref} = -\,[\Delta A(F/W_o) + \Delta B(\zeta_{ref})] \tag{20}$$

Changes in λ due to variations in I_{sp}, for a given value of f_e, can be expressed as

$$(\Delta\lambda)_I = (\lambda_{ref})_I - \lambda_{ref} \tag{21}$$

Calculations were made varying I_{sp} in increments of 25 sec over the range considered. The changes in payload ratio were computed using equation 21 and are shown in Figure 8. While the curves are irregular and intersecting, linear interpolation for both f_e I_{sp} is sufficiently accurate.

The values of $\Delta\lambda_I$ are independent of the vehicle specific weight parameters assumed, but are remotely dependent upon initial altitude. However, it was found that within the altitude range considered, this dependency of $\Delta\lambda_I$ can be neglected. In other words, equation 21 can be expressed as

$$\Delta\lambda_I = (\lambda_{ref})_{I,h_o} - (\lambda_{ref})_{h_o}$$

and yield approximately the same results as shown in Figure 8.

Changes in the initial orbit altitude, other reference conditions remaining constant, must also be accounted for in estimating payload ratio. It was fortuitously discovered that the change in payload for an incremental change in altitude is approximately the same over the range of altitudes considered, regardless of the value of the specific impulse. Consequently, altitude and specific impulse corrections to the reference payload ratio can be made independently. The same applies to the other performance parameters.

It was found convenient in this report to base altitude correction on a 100-N. M. incremental decrease in altitude. The change in reference payload ratio for an incremental decrease of 100 N. M. is shown in Figure 9. Again linear interpolation for f_e is sufficient, since altitude corrections are generally small. For arbitrary initial altitude, h_o, the change in payload is given by

$$\Delta\lambda_{h_o} = \frac{(h_o)_{ref} - h_o}{100} (\Delta\lambda_{h_o})_{100}$$

$$= \frac{300 - h_o}{100} (\Delta\lambda_{h_o})_{100} \qquad (22)$$

where $(\Delta\lambda_{h_o})_{100}$ is the correction shown in Figure 9, and $(h_o)_{ref}$ and h_o are measured in nautical miles.

Combining the corrections represented by equations 20, 21 and 22, the payload ratio for any assumed set of conditions can be found from

$$(\lambda)_{A, B, I, h_o} = \lambda_{ref} + \Delta\lambda_{A, B} + \Delta\lambda_I + \Delta\lambda_{h_o}$$

Furthermore, for non-zero values of C, this becomes

$$(\lambda)_{A, B, C, I, h_o} = \lambda_{ref} + (\Delta\lambda)_{A, B} + \Delta\lambda_I + \Delta\lambda_{h_o} - C \qquad (23)$$

Using this relation, the payload ratio for a particular vehicle with a given mission can be computed. Repeating the procedure for various values of F/W_o, curves such as those shown in Figure 1 may be constructed, and the F/W_o for maximum payload ratio determined. More will be said later concerning the payload ratio curves. Several numerical examples are included in the Appendix, illustrating the performance estimation procedures.

Characteristic Velocity

The characteristic velocity, ΔV_{id}, representing a combination of the inertial velocity requirement and gravity losses, is computed in a manner similar to that described for estimating payload ratio. Reference characteristic velocity curves are shown in Figure 2. The change in reference characteristic velocity for nonreference specific impulses, $\Delta(\Delta V_{id})_I$, is shown in Figure 10. Because of the small variation of

ΔV_{id} with I_{sp}, curves are shown only for 700, 900 and 1000 sec. These corrections were computed from the relation

$$\Delta(\Delta V_{id})_I = [(\Delta V_{id})_{ref}]_I - (\Delta V_{id})_{ref} \tag{24}$$

which is analagous to equation 21.

The change in reference characteristic velocity for an incremental altitude decrease of 100 N. M. is shown in Figure 11. Analagous to equation 22, the change in ΔV_{id} for arbitrary initial altitudes is given by

$$\begin{aligned}(\Delta V_{id})_{h_o} &= \frac{(h_o)_{ref} - h_o}{100} \left[\Delta(\Delta V_{id})_{h_o}\right]_{100} \\ &= \frac{300 - h_o}{100} \left[\Delta(\Delta V_{id})_{h_o}\right]_{100}\end{aligned} \tag{25}$$

with $\left[\Delta(\Delta V_{id})_{h_o}\right]_{100}$ determined from Figure 11.

The characteristic velocity for arbitrary values of I_{sp} and h_o is then given by

$$(\Delta V_{id})_{I, h_o} = (\Delta V_{id})_{ref} + \Delta(\Delta V_{id})_I + \Delta(\Delta V_{id})_{h_o} \tag{26}$$

Propellant Ratio

The propellant ratio, ζ, can be estimated in a manner similar to that described for payload ratio and characteristic velocity. However, once ΔV_{id} is determined for the desired conditions, it is easier and faster to calculate ζ using equation 13. Hence,

$$(\Delta V_{id})_{I, h_o} = g_n I_{sp} \ln \frac{1}{1 - (\zeta)_{I, h_o}}$$

or

$$(\zeta)_{I, h_o} = 1 - \exp\left[\frac{-(\Delta V_{id})_{I, h_o}}{g_n I_{sp}}\right] \tag{27}$$

While the reference curves for ζ shown in Figure 3 are not used here, the curves are needed to determine ζ_{ref} for equation 20.

Burning Time

Following the calculation of ζ, burning time to injection is readily determined from equation 12 in the form

$$(t_b)_{I,h_o} = \frac{I_{sp}(\zeta)_{I,h_o}}{(F/W_o)} \tag{28}$$

Burning time curves for reference conditions are not used in the estimation procedure but are shown in Figure 4, for the purpose of illustrating the typical variation with F/W_o and f_e.

Flight Path Angle and Central Angle

The procedure for estimating the flight path angle, θ, and the central angle, ψ, is identical to the procedure outlined for calculating ΔV_{id} and they are discussed together. Thus analagous to equations 24 and 25, the change of θ and ψ with I_{sp} is given by

$$(\Delta\theta)_I = (\theta_{ref})_I - \theta_{ref} \tag{29}$$

and

$$(\Delta\psi)_I = (\psi_{ref})_I - \psi_{ref} \tag{30}$$

These corrections are shown in Figure 12 and 14, respectively.

The change of θ and ψ for arbitrary h_o is determined from the relations

$$(\Delta\theta)_{h_o} = \frac{300 - h_o}{100} (\Delta\theta_{h_o})_{100} \tag{31}$$

$$(\Delta\psi)_{h_o} = \frac{300 - h_o}{100} (\Delta\psi_{h_o})_{100} \tag{32}$$

where $(\Delta\theta_{h_o})_{100}$ and $(\Delta\psi_{h_o})_{100}$, the corrections for a 100-N.M. decrease in initial altitude, are given in Figure 13 and 15 respectively. Equations 31 and 32 are analagous to equation 25 and follow a similar development. It should be noted that the sign of $(\Delta\theta_{h_o})_{100}$ in Figure 13 can be positive or negative. Care should be exercised to insure that the proper sign, corresponding to the appropriate value of F/W_o, is used in equation 31.

It follows that, for arbitrary conditions

$$(\theta)_{I, h_o} = \theta_{ref} + (\Delta\theta)_I + (\Delta\theta)_{h_o} \tag{33}$$

and

$$(\psi)_{I, h_o} = \psi_{ref} + (\Delta\psi)_I + (\Delta\psi)_{h_o} \tag{34}$$

Altitude at Injection

The exact altitude at injection is usually of little interest in preliminary studies. Consequently, in this report, the injection altitude is approximated by

$$(h_b)_{I, h_o} = (h_b)_{ref} + [h_o - (h_o)_{ref}] \tag{35}$$

or

$$(h_b)_{I, h_o} = (h_b)_{ref} + (h_o - 300) \tag{36}$$

As will be seen later in the numerical examples, the per cent error involved in estimating h_b with equation 36 is much larger than the error associated with the other performance parameters. If more exacting accuracy is desired, the procedure of computing changes due to variations in h_o and I_{sp} used for ψ, θ and ΔV_{id} can be applied

ASSUMPTIONS

The basic assumptions made in the analysis are summarized as follows:

1. Acceleration of a single stage out of a circular earth orbit, with constant tangential thrust, to the required hyperbolic excess speed

2. Range of independent performance parameters:

I_{sp} = 700 - 1000 sec

f_e = 0 - 0.5

h_o = 100 - 400 N.M. (185.3 - 741.2 km)

F/W_o = 0.04 - 0.50

3. Reference conditions:

I_{sp} = 800 sec

h_o = 300 N.M. (555.0 km)

A = B = 0.10

C = 0

4. Mean spherical earth model with

$\mu_{\oplus} = 62,698 \frac{\text{N.M.}^3}{\text{sec}^2}$ $\left(398,613 \frac{\text{km}^3}{\text{sec}^2}\right)$

$r_{\oplus}$ = 3438.3 N.M. (6371.1 km)

$V_{\oplus}$ = 29,770 m/sec

DISCUSSION OF RESULTS

Several numerical examples are included in the Appendix to illustrate the performance estimation procedure and its associated accuracy. Complete details of the estimation procedure are given for two of the examples, while only results are shown for the others. One example is included with a parameter (initial orbital altitude) outside the range assumed earlier as a means of determining the accuracy with which the parametric data can be extrapolated.

The assumed vehicle characteristics and hyperbolic excess requirements of the numerical examples are listed in Table 1. Conditions were deliberately chosen such that interpolation on the various graphs was necessary in most cases. Hence, the results should be indicative of the maximum errors which can be expected in practical

applications of the estimation procedure. A comparison of the various performance parameters is shown in Table 2. Maximum and average errors obtained in the examples are also presented in this table. The examples are not numerous enough, by any means, to represent a statistical sampling; hence the errors shown should not be construed as being the most probable.

Some discussion is in order concerning payload ratio since this parameter is frequently misinterpreted. Curves of payload ratio, such as those shown in Figure 1 can be used in several ways. If a particular vehicle system and mission profile are assumed so that values of A, B, C, I_{sp}, h_o and f_e are specified, payload ratio can be calculated over a range of f/W_o. Consider for example the conditions assumed in Example 1 of the Appendix. Payload ratio as a function of F/W_o for this case is shown in Figure 16. Maximum payload ratio is seen to occur at an F/W_o of approximately 0.25.

It must be emphasized, however, that maximum payload ratio and maximum payload do not necessarily occur at the same F/W_o. To illustrate this point, it is necessary to examine three possible cases concerning the values of F and W_o. These are as follows:

1. Both F and W_o fixed
2. W_o fixed but F variable
3. F fixed but W_o variable.

If both F and W_o are fixed, as in the first case, a particular value F/W_o, and hence λ, is specified. Referring to Figure 16 again, suppose that F = 50,000 pounds and W_o = 200,000 pounds so that F/W_o = 0.25 corresponding to λ = 0.2500, the optimum value. The payload can then be determined from the relation

$$W_{gd} = \lambda W_o$$

Thus,

$$W_{gd} = (0.2500)\ (200,000) = 50,000 \text{ lb}$$

Consider now the second case, where W_o is fixed but F is variable. Each value of F/W_o in Figure 16 now corresponds to a different value of F. It is readily apparent, however, that no other value of F will yield a higher payload than the value assumed in Case 1 above. For example, assume F = 20,000 pounds; then F/W_o = 0.10 and λ is seen to be equal to 0.2142 and thus,

$$W_{gd} = (0.2142)\ (200,000) = 42,840 \text{ lb}$$

which is indeed a decrease in payload. If other values of F are assumed and the resulting payloads are determined in a similar manner, a plot of payload versus F/W_o would have the same shape as the λ curve. Thus, in the second case, no matter what fixed value of W_o is assumed, maximum payload and maximum payload ratio occur at the same F/W_o.

Consider, however, the third case where F is fixed and W_o is variable. This case is analagous to the mating of a given engine system to various initial weights in orbit, each value of F/W_o representing a different W_o. Thus for F fixed at 50,000 pounds, assume that W_o is 500,000 pounds so that F/W_o and λ are the same as in Case 2 above. The payload now, however, is

$$W_{gd} = (0.2142)\ (500,000) = 107,100 \text{ lb}$$

or more than twice the value obtained with the same engine in Case 1 above at maximum payload ratio. If other values of W_o, and hence F/W_o, are assumed the payload curve is as shown in Figure 16. This curve is seen to be entirely different from the payload ratio curve in shape. Furthermore, it appears from Figure 16 that the payload increases continuously as F/W_o becomes small. In other words, as the initial weight in orbit increases as indicated by the tick-marks on the payload curve, the payload increases accordingly. It should be remembered however that the low values of F/W_o correspond to extremely long burning times.

Suppose now, however, that a higher hyperbolic excess speed is required of the engine system assumed above. Figure 17 shows payload and payload ratio curves for an f_e of 0.46, as opposed to the 0.29 value assumed in Figure 16. Tick-marks corresponding to the same initial weights denoted in Figure 16 are shown on the payload curve of Figure 17. Rather than increasing continuously as before, the payload curve now has a maximum point occurring at an F/W_o of 0.108 (W_o = 462,963 lb). Note also that this maximum point does not occur at the same F/W_o as the maximum payload ratio.

The next question is why is there an optimum on the payload curve? The answer, while not so obvious at first glance, can be found by considering the velocity requirement, ΔV_{id}. If one constructed curves of ΔV_{id} as a function of F/W_o for f_e values of 0.29 and 0.46 and the other assumptions made for I_{sp}, h_o, A, B and C, the curve for f_e = 0.46 would have a greater slope and consequently a greater change in ΔV_{id} for a given change in F/W_o (see Fig. 2 for an indication). In going from W_o = 500,000 lb to W_o = 1,000,000 lb in Figure 16 and 17, F/W_o is halved. In Figure 16, the gain in initial weight is more than enough to overcome the resulting increase in ΔV_{id}. The opposite is true in Figure 17 where the increase in ΔV_{id} is so large that the increase in W_o is not enough to overcome the additional propellant and tankage weights required. It should be noted in Figure 17 that the λ curve becomes zero within the range of F/W_o considered. This is not the case in Figure 16.

For the lower hyperbolic excess velocities, maximum payload occurs at extremely low values of F/W_o which are impractical because of the long burning times and/or large initial weights required. The lowest value of f_e for which a maximum payload falls within a practical range of F/W_o can be determined by the trial and error process of assuming values of f_e and calculating the payload curves. The magnitude of this value of f_e is of course dependent upon I_{sp}, h_o, A and B. Higher values of f_e tend to shift maximum payload toward higher values of F/W_o.

The possibility of a maximum payload for a particular mission is extremely important in interplanetary operations if the mission must be made with an existing or predefined engine system. For the case considered in Figure 17, for example, it would be absurd to assemble 1,000,000 lb in orbit when more payload could be achieved with an initial weight of 250,000 lb, and with far less burning time. The reduction in earth launch vehicle capability is evident.

If the desired mission requires more payload than the maximum attainable with a specific engine, a higher thrust is in order and the payload ratio curves can be used to determine the desirable thrust level. If in a particular case the engine cannot withstand the burning time required to achieve the maximum payload, the greatest payload possible then obviously corresponds to the F/W_o which yields the limiting burning time.

CONCLUSIONS

Based on the results of the numerical examples in the Appendix, it can be concluded that the methodology presented in this report for estimating trajectory characteristics and vehicle performance is rapid, unsophisticated and practical. Performance estimations can be made for any vehicle system and mission profile, within the range assumed for the various associated parameters. Use of the procedure and data presented allows a quick determination of propulsion requirements for specific mission profiles. The approach used can be extended to cover a wider range of the independent parameters including, for example, those typical of conventional chemical systems.

The errors shown in Table 2 are indicative of the average and maximum errors which can be expected in a particular application of the estimation procedure. Based on the results of examples 1 through 4, it can be conservatively concluded that the maximum errors associated with careful estimation of the various performance parameters are as follows:

λ, ζ, ΔV_{id}, t_b - - - - - - - - - < 1%

θ, ψ - - - - - - - - - < 3%

h_b - - - - - - - - - <15%

These errors are well within the range usually required of preliminary design ıdies. It was pointed out earlier that the burnout altitude can be determined more ɔurately if desired.

From the discussion earlier, it can be concluded that, for certain hyperbolic ɔess velocities, there is an otpimum initial weight in orbit when operating with a ed engine system. However, this optimum does not generally yield the maximum yload ratio. In many cases, the F/W_0 for optimum payload may require burning nes of which the engine may not be capable. In such cases, the maximum payload ainable corresponds to the F/W_0 which yields the limiting burning time. In any ent, the possibility of a maximum payload for a particular mission and engine system extremely important in interplanetary operations.

Finally from the discussion earlier, the following general conclusions can be ade:

1. If both F and W_0 are fixed, the procedure presented can be readily applied determine the resulting performance parameters for a given mission.

2. If W_0 is fixed but F (and hence the engine system) is variable, the W_0 for aximum payload and maximum payload ratio is the same.

3. If F is fixed but W_0 is variable, the F/W_0 for maximum payload can be termined and is usually lower than the F/W_0 for maximum payload ratio.

APPENDIX

NUMERICAL EXAMPLES

The purpose of this Appendix is to illustrate numerically the procedures outlined in the text of this report. Five examples are considered, with two being worked out in detail. Only results are shown for the remaining three. The data assumed for all examples are listed in Table 1.

Example Number 1

The first step in making a performance estimation is the determination of reference values, since these constitute a basis for the estimation procedure. The necessary reference values for Example 1, corresponding to the arbitrarily assumed values for $F/W_o = 0.2$ and $f_e = 0.29$, can be read from Figure 1 (a,b), 2b, 3, 5, 6 and 7 as follows:

$$\lambda_{ref} = 0.3359$$

$$\zeta_{ref} = 0.5880$$

$$(\Delta V_{id})_{ref} = 6940 \text{ m/sec}$$

$$\theta_{ref} = 40.5^\circ$$

$$\psi_{ref} = 130.0^\circ$$

$$(h_b)_{ref} = 4641 \text{ N.M.}$$

The most important performance parameter to be estimated is payload ratio, λ. As discussed in the text, it is necessary to correct λ_{ref} for changes in A, B, C, I_{sp} and h_o. For A = 0.20 and B = 0.15 (from Table 1) equations 18 and 19 yield

$$\Delta A = A - 0.10$$

$$= 0.20 - 0.10$$

$$= 0.10$$

$$\Delta B = B - 0.10$$

$$= 0.15 - 0.10$$

$$= 0.05$$

From equation 20, the change in λ_{ref} due to non-reference values of A and B is

$$\Delta\lambda_{A,B} = - [\Delta A\,(F/W_o) + \Delta B\,(\zeta_{ref})]$$

$$= - [0.10(0.20) + 0.05(.5880)]$$

$$= - 0.0494$$

The change in λ_{ref} due to the change in I_{sp} can be determined by linear interpolation between Figure 8b and 8c. Hence, for $I_{sp} = 735$ sec and $f_e = 0.29$

$$\Delta\lambda_I = -0.0326$$

The change in λ_{ref} due to change in h_o is found from Figure 9 and equation 22. From Figure 9,

$$(\Delta\lambda_{h_o})_{100} = -0.0032$$

It follows from equation 22 that

$$\Delta\lambda_{h_o} = \frac{300 - h_o}{100}\,(\Delta\lambda_{h_o})_{100}$$

$$= \frac{300 - 150}{100}\,(-0.0032)$$

$$= -0.0048$$

Finally, the payload ratio for the desired conditions can be found from equation 23,

$$\lambda = \lambda_{ref} + \Delta\lambda_{A,B} + \Delta\lambda_I + \Delta\lambda_{h_o} - C$$

$$= 0.3359 - 0.0494 - 0.0326 - 0.0048 - 0$$

$$= 0.2491$$

The characteristic velocity requirement is determined in a similar manner. The specific impulse correction to $(\Delta V_{id})_{ref}$ is found from Figure 10a. For an I_{sp} of 700 sec, the figure shows that

$$\Delta(\Delta V_{id})_I = -44 \text{ m/sec}$$

Hence for an I_{sp} of 735 sec, remembering that $(I_{sp})_{ref} = 800$ sec,

$$\Delta(\Delta V_{id})_I = \frac{800 - 735}{800 - 700} (-44)$$

$$= 0.65 (-44)$$

$$= -28.6 \text{ m/sec}$$

The initial altitude correction is found from Figure 11 and equation 25. From Figure 11,

$$[\Delta(\Delta V_{id})_{h_o}]_{100} = 55.0 \text{ m/sec}$$

and equation 25 gives

$$\Delta(\Delta V_{id})_{h_o} = \frac{300 - h_o}{100} [\Delta(\Delta V_{id})]_{100}$$

$$= \frac{300 - 150}{100} (55.0)$$

$$= 82.5 \text{ m/sec}$$

Finally, from equation 26,

$$\Delta V_{id} = (\Delta V_{id})_{ref} + \Delta(\Delta V_{id})_I + \Delta(\Delta V_{id})_{h_o}$$

$$= 6940.0 - 28.6 + 82.5$$

$$= 6993.9 \text{ m/sec}$$

The propellant ratio is readily determined from equation 27 as follows,

$$\zeta = 1 - \exp\left[\frac{-(\Delta V_{id})_{I, h_o}}{g_n I_{sp}}\right]$$

$$= 1 - \exp\left[-\frac{6993.9}{9.82(735)}\right]$$

$$= 0.6207$$

The burning time follows from equation 28,

$$t_b = \frac{I_{sp}(\zeta)_{I,h_o}}{F/W_o}$$

$$= \frac{735(0.6207)}{0.20}$$

$$= 2281.1 \text{ sec}$$

The specific impulse correction to the reference flight path angle is determined from Figure 12a, for $I_{sp} = 700$ sec, to be,

$$(\Delta\theta)_I = 1.7°$$

Thus, for $I_{sp} = 735$ sec,

$$(\Delta\theta)_I = 0.65\,(1.7)$$

$$= 1.1°$$

The altitude correction to θ_{ref} is found from Figure 13 and equation 31. From Figure 13,

$$(\Delta\theta_{h_o})_{100} = -0.55°$$

Equation 31 then gives,

$$\Delta\theta_{h_o} = \frac{300 - h_o}{100}(\Delta\theta_{h_o})_{100}$$

$$= \frac{300 - 150}{100}(-0.55)$$

$$= -0.8°$$

The predicted value of θ is then determined from equation 33,

$$\theta = \theta_{ref} + (\Delta\theta)_I + (\Delta\theta)_{h_o}$$

$$= 40.5^\circ + 1.1^\circ - 0.8^\circ$$

$$= 40.8^\circ$$

The central angle ψ is determined in an identical manner using Figure 14a and 15, and equation 34 with the results:

$$\Delta\psi_I = -1.6^\circ$$

$$\Delta\psi_{h_o} = 5.4^\circ$$

and hence,

$$\psi = \psi_{ref} + \Delta\psi_I + \Delta\psi_{h_o}$$

$$= 130.0 - 1.6 + 5.4$$

$$= 133.8^\circ$$

The final performance parameter is burnout altitude, which is estimated by use of equation 36 which gives,

$$h_b = (h_b)_{ref} + (h_o - 300)$$

$$= 4641 + (150 - 300)$$

$$= 4491 \text{ N. M.}$$

The values estimated for each of the performance parameters in Example 1 are recorded in Table 2 where they are compared with the actual computer solution of the same problem. The errors associated with the estimated values are less than one per cent for all parameters except burnout altitude.

Example Number 2

The specified conditions for Example 2 are given in Table 1. The necessary reference values, corresponding to $F/W_o = 0.10$ and $f_e = 0.35$, can be read from Figure 1c, 2c, 5, 6, and 7 as follows:

$$\lambda_{ref} = 0.2220$$

$$\zeta_{ref} = 0.7000$$

$$(\Delta V_{id})_{ref} = 9400 \text{ m/sec}$$

$$\theta_{ref} = 25.1^\circ$$

$$\psi_{ref} = 196.0^\circ$$

$$(h_b)_{ref} = 14030 \text{ N.M.}$$

For $A = 0.08$ and $B = 0.07$, equations 18 and 19 give,

$$\Delta A = A - 0.10$$

$$= 0.07 - 0.10$$

$$= -0.02$$

$$\Delta B = B - 0.10$$

$$= 0.07 - 0.10$$

$$= -0.03$$

If follows from equation 20 that,

$$(\Delta\lambda)_{A,B} = -[\Delta A(F/W_o) + \Delta B(\zeta_{ref})]$$

$$= -[(-0.02)(0.10) + (-0.03)(0.7000)]$$

$$= 0.0230$$

Linear interpolation between Figure 8g and 8h gives the specific impulse correction,

$$\lambda_I = 0.0375$$

From Figure 9,

$$(\Delta\lambda_{h_o})_{100} = -0.0039$$

and equation 22 gives the initial altitude correction,

$$\Delta\lambda_{h_o} = \frac{300 - h_o}{100} (\Delta\lambda_{h_o})_{100}$$

$$= \frac{300 - 375}{100} (-0.0039)$$

$$= 0.0029$$

The desired value of λ is then found from equation 23,

$$\lambda = \lambda_{ref} + \Delta\lambda_{A,B} + \Delta\lambda_I + \Delta\lambda_{h_o} - C$$

$$= 0.2220 + 0.0230 + 0.0375 + 0.0029 - 0.01$$

$$= 0.2754$$

The specific impulse correction to $(\Delta V_{id})_{ref}$ is found from Figure 10b. For an I_{sp} of 900 sec, the figure shows that

$$\Delta(\Delta V_{id})_I = -69.0 \text{ m/sec}$$

Hence for an I_{sp} of 885 sec,

$$\Delta(\Delta V_{id})_I = 0.85(-69.0)$$

$$= -58.7 \text{ m/sec}$$

The initial altitude correction is found from Figure 11 and equation 25. From Figure 11,

$$[\Delta(\Delta V_{id})_{h_o}]_{100} = 92.0 \text{ m/sec}$$

and equation 25 gives,

$$\Delta(\Delta V_{id})_{h_o} = \frac{300 - h_o}{100} \left[\Delta(\Delta V_{id})\right]_{100}$$

$$= 9400.0 - 58.7 + 69.0$$

$$= 9410.3 \text{ m/sec}$$

The propellant ratio follows from equation 27,

$$\zeta = 1 - \exp\left[\frac{-(\Delta V_{id})_{I, h_o}}{g_n I_{sp}}\right]$$

$$= 1 - \exp\left[\frac{-9410.3}{9.82\,(885)}\right]$$

$$= 0.6614$$

Burning time can then be calculated from equation 28,

$$t_b = \frac{I_{sp}(\zeta)_{I, h_o}}{F/W_o}$$

$$= \frac{885(0.6614)}{0.1}$$

$$= 5853.4 \text{ sec}$$

The specific impulse correction to the reference flight path angle is determined from Figure 12b, for $I_{sp} = 700$ sec, to be

$$(\Delta\theta)_I = -1.17°$$

Thus, for $I_{sp} = 885$ sec,

$$(\Delta\theta)_I = 0.85\,(-1.17)$$

$$= -1.0^\circ$$

The altitude correction to θ_{ref} is found from Figure 13 and equation 31. From Figure 13,

$$(\Delta\theta_{h_o})_{100} = -0.05^\circ$$

Equation 31 then gives,

$$\Delta\theta_{h_o} = \frac{300 - h_o}{100}\,(\Delta\theta_{h_o})_{100}$$

$$= \frac{300 - 375}{100}\,(-0.05)$$

$$\approx 0.0^\circ$$

The desired value of θ is then determined from equation 33,

$$\theta = \theta_{ref} + \Delta\theta_I + \Delta\theta_{h_o}$$

$$= 25.1 - 1.0 + 0$$

$$= 24.1^\circ$$

From Figure 14b and 15, and equation 34, the specific impulse and altitude corrections to ψ_{ref} are found to be,

$$\Delta\psi_I = 2.5^\circ$$

$$\Delta\psi_{h_o} = -3.8^\circ$$

Hence,

$$\psi = \psi_{ref} + \Delta\psi_I + \Delta\psi_{h_o}$$

$$= 196.0 + 2.5 - 3.8$$

$$= 194.7^\circ$$

Finally, from equation 36, the burnout altitude is estimated to be,

$$h_b = (h_b)_{ref} + (h_o - 300)$$

$$= 14030 + (375 - 300)$$

$$= 14105 \text{ N. M.}$$

The results of Example 2 are summarized in Table 2 and compared with the exact values. The results of the remaining examples assumed in Table 1 are also included in Table 2. Example 5 assumes an initial altitude (h_o = 525 N. M.) which is outside the range considered. The resulting errors are comparable with those obtained in the other examples except for the error associated with payload ratio. This would indicate that equation 22 is not as accurate for the higher altitudes.

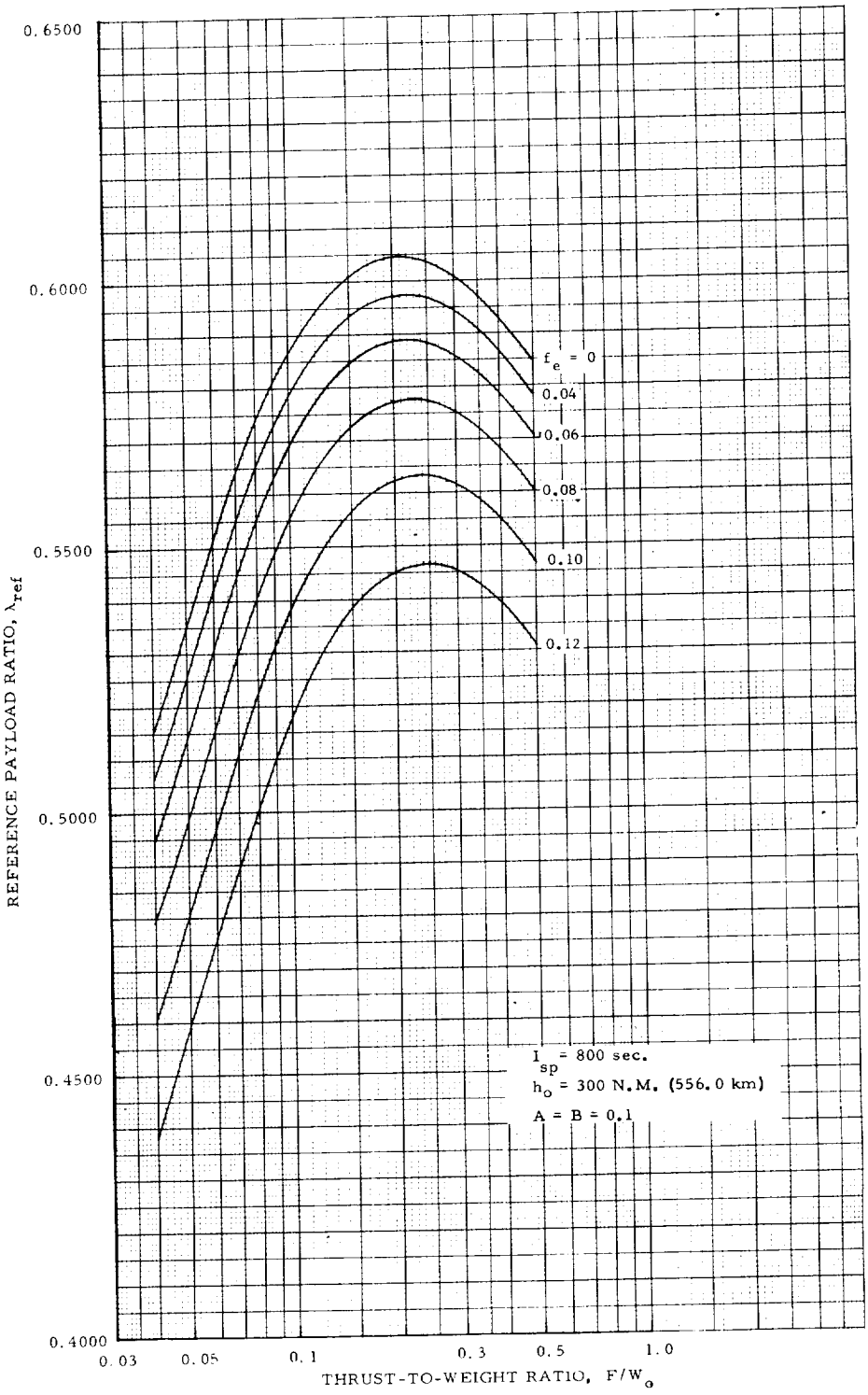

1a. REFERENCE PAYLOAD RATIO FOR HYPERBOLIC EXCESS REQUIREMENTS f_e = 0 to f_e = 0.12

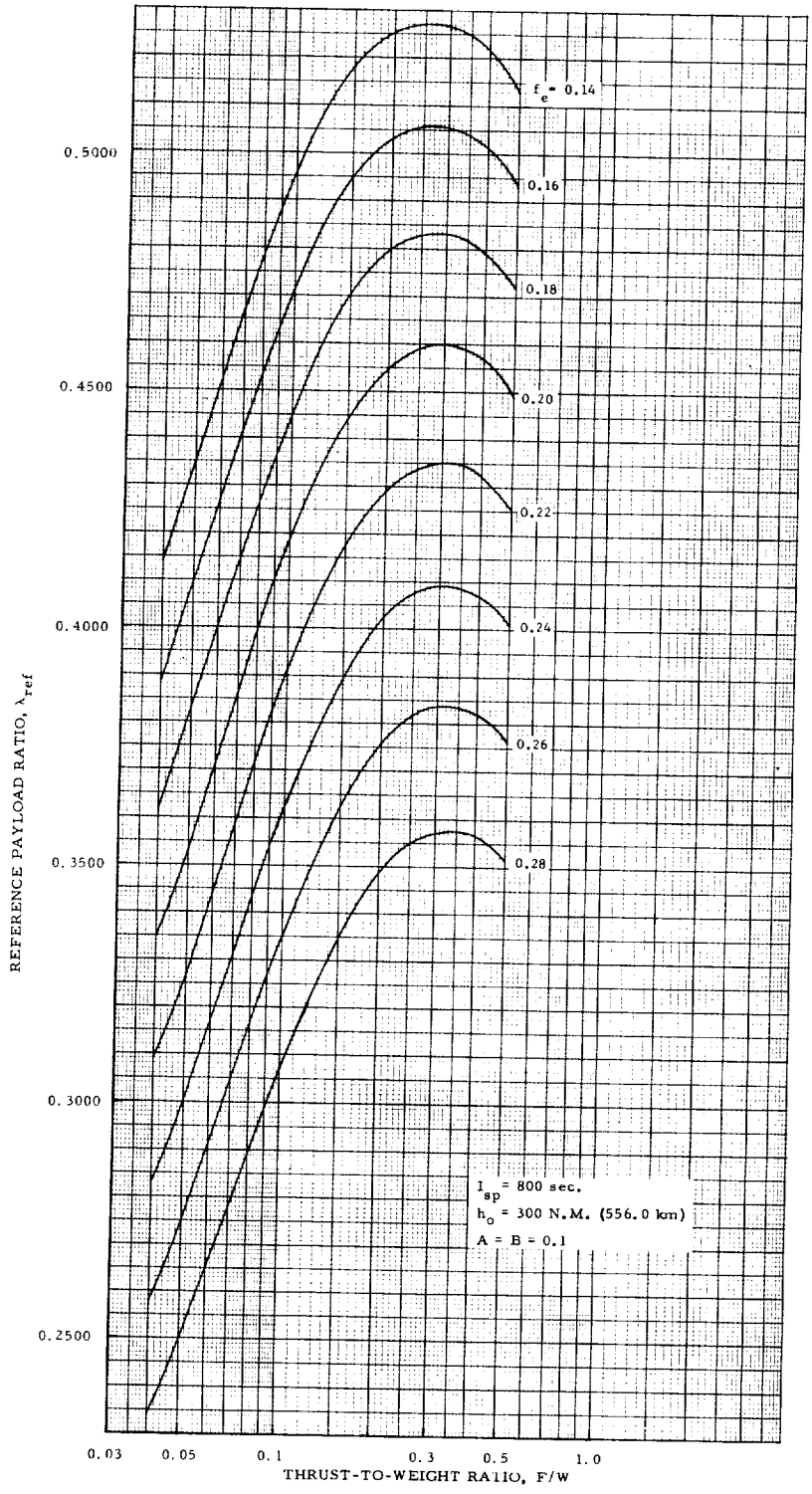

FIGURE 1b. REFERENCE PAYLOAD RATIO FOR HYPERBOLIC EXCESS REQUIREMENTS f_e = 0.14 to f_e = 0.28

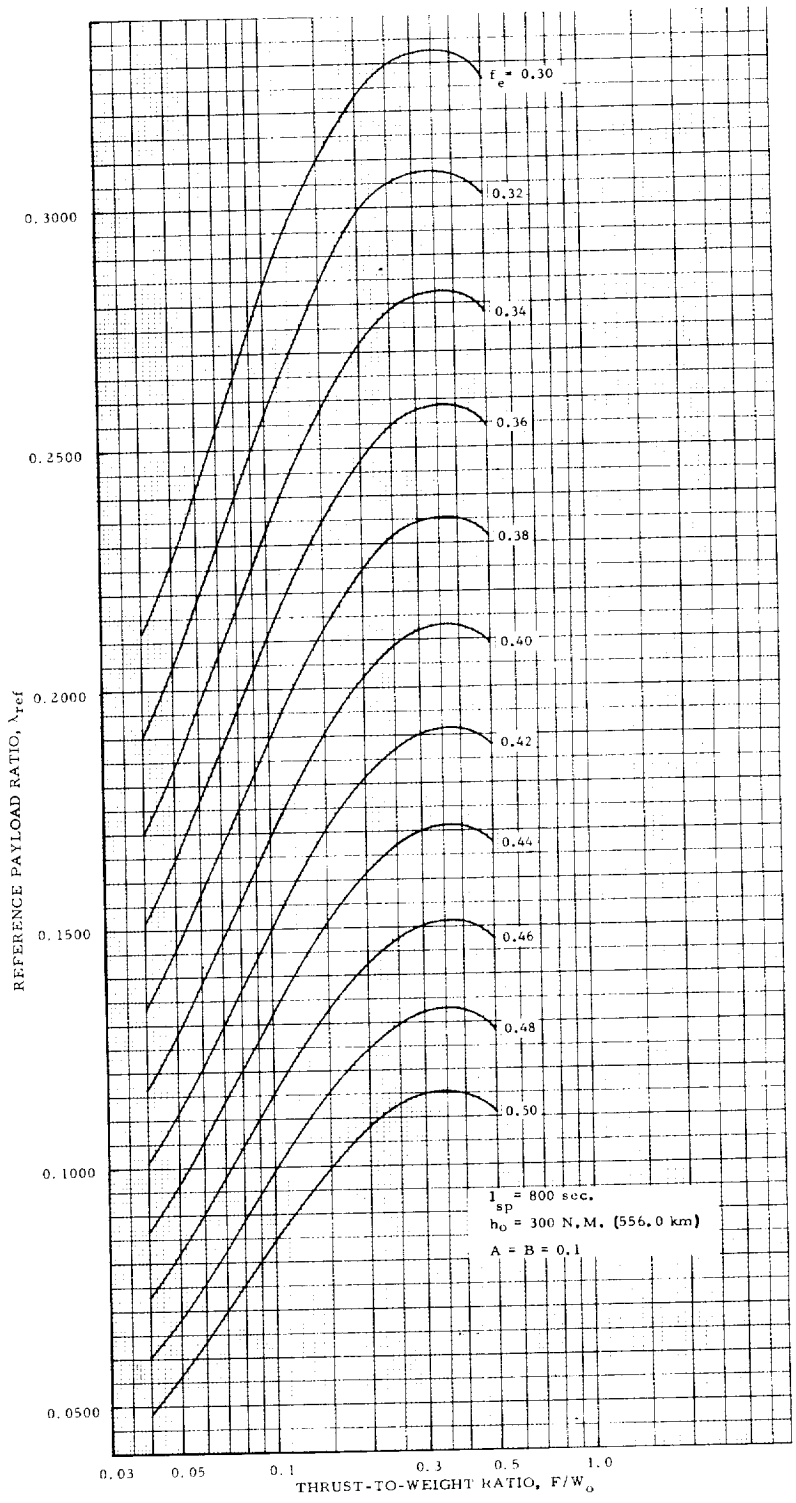

FIGURE 1c. REFERENCE PAYLOAD RATIO FOR HYPERBOLIC EXCESS REQUIREMENTS f_e = 0.30 to f_e = 0.50

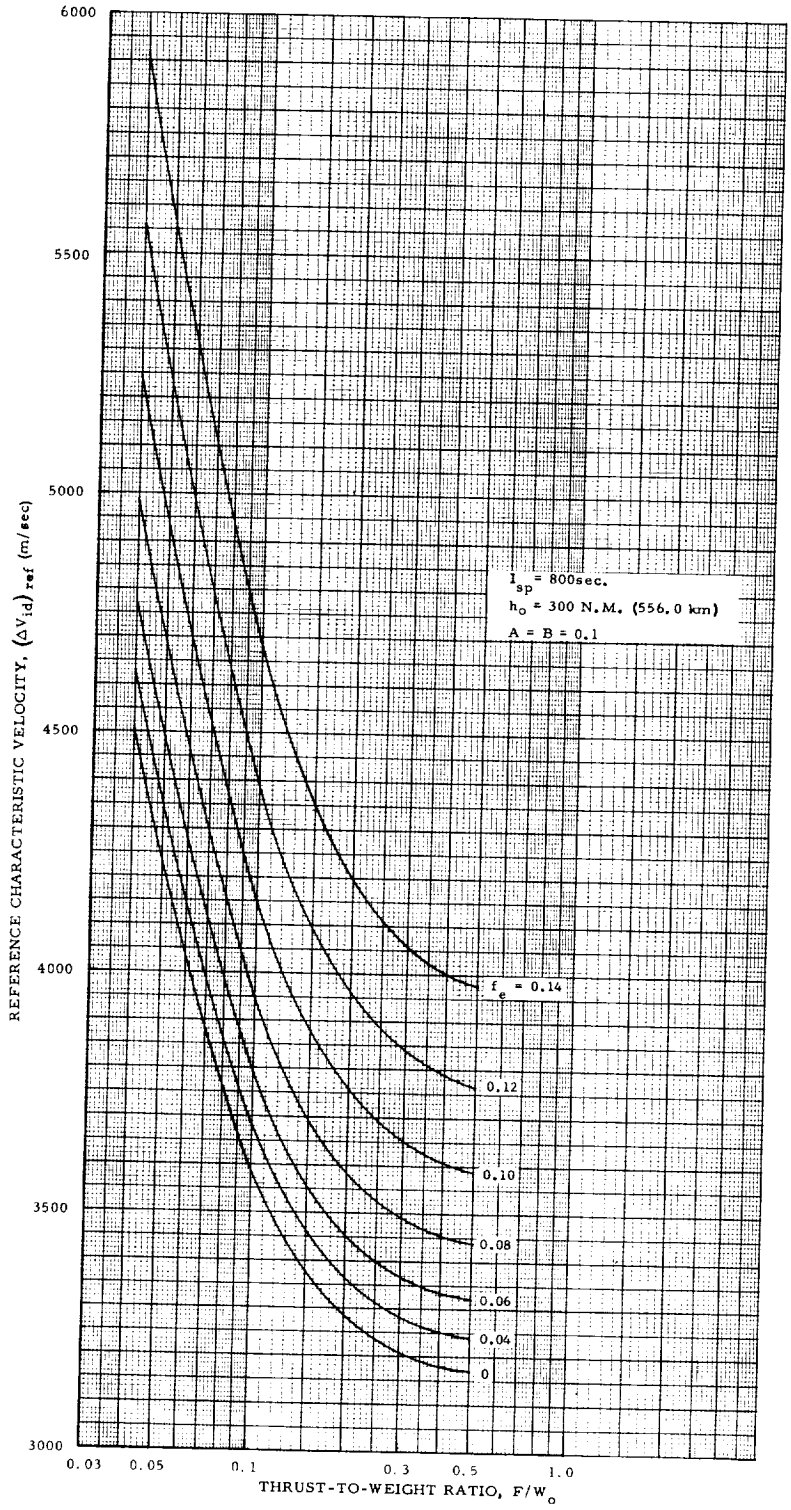

FIGURE 2a. REFERENCE CHARACTERISTIC VELOCITY FOR HYPERBOLIC EXCESS REQUIREMENTS $f_e = 0$ to $f_e = 0.14$

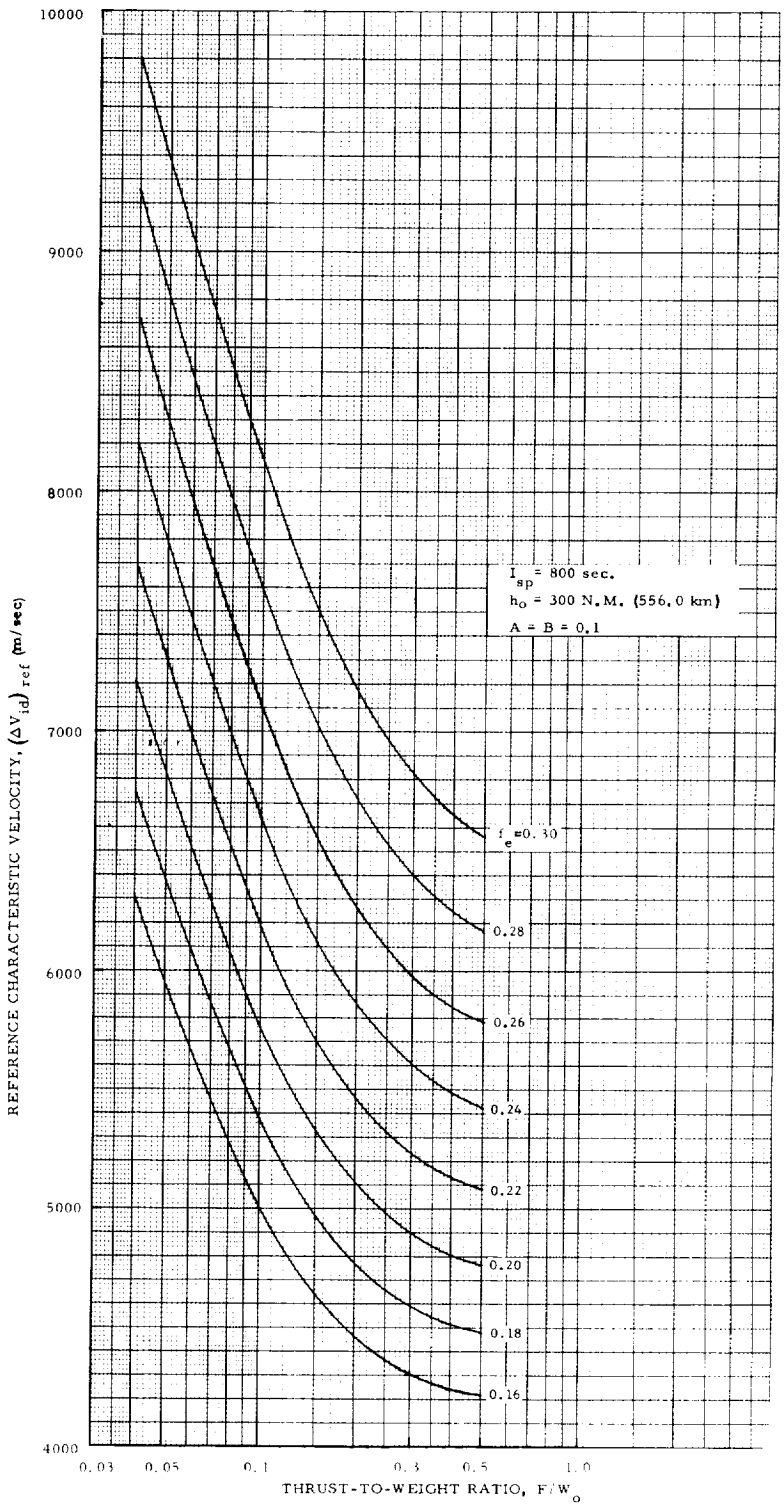

FIGURE 2b. REFERENCE CHARACTERISTIC VELOCITY FOR HYPERBOLIC EXCESS REQUIREMENTS f_e = 0.16 to f_e = 0.30

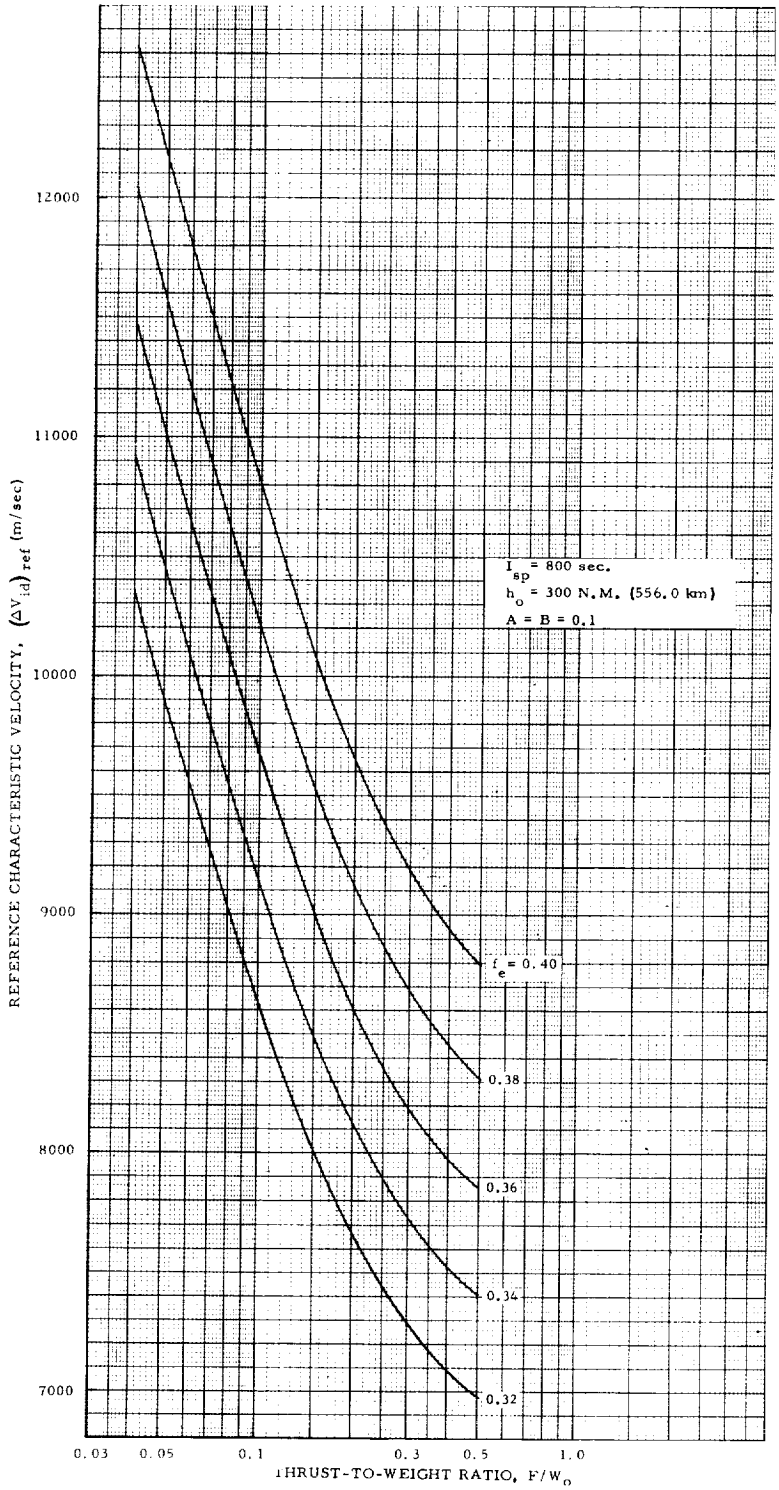

FIGURE 2c. REFERENCE CHARACTERISTIC VELOCITY FOR HYPERBOLIC EXCESS REQUIREMENTS $f_e = 0.32$ to $f_e = 0.40$

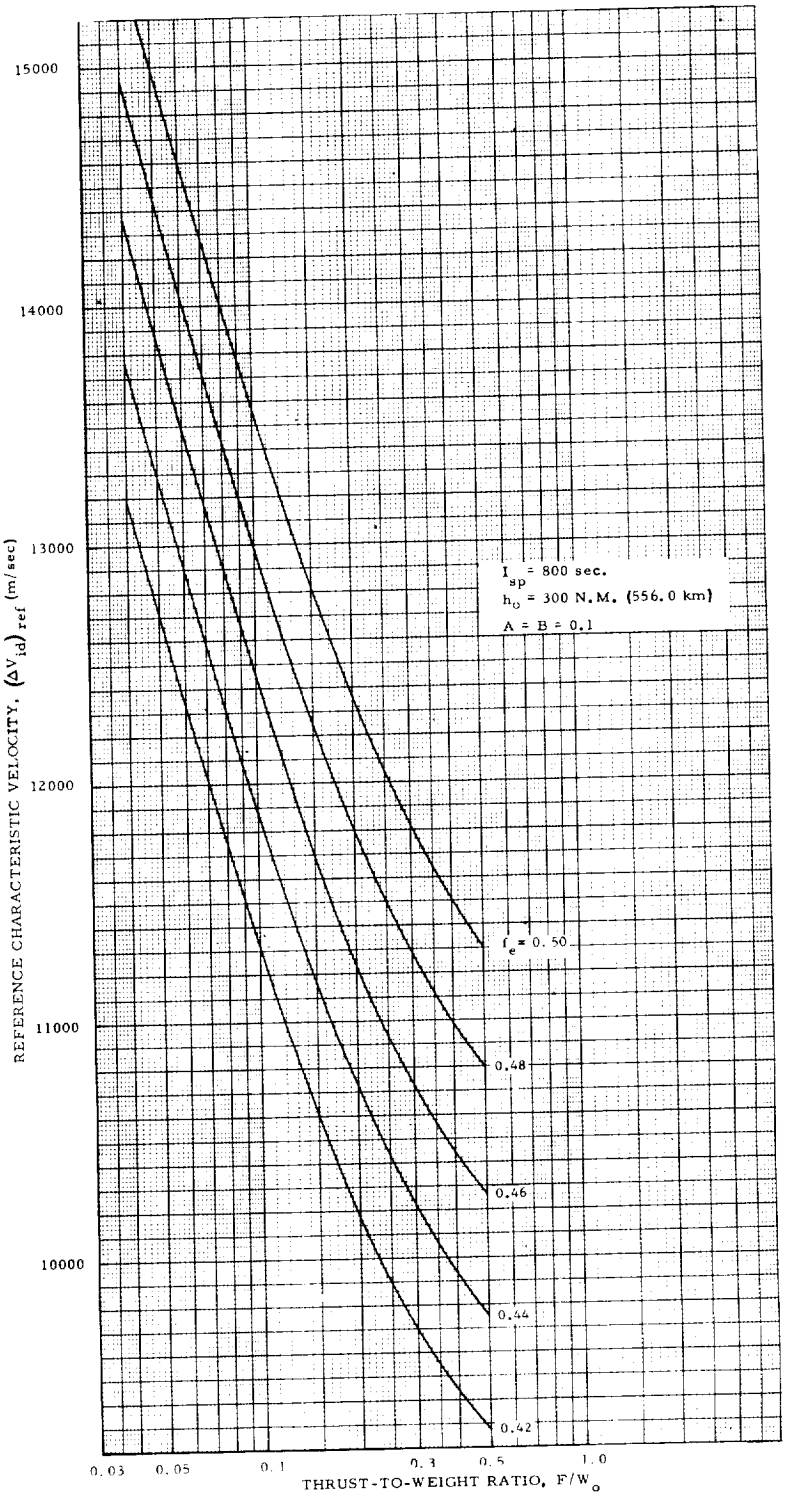

FIGURE 2d. REFERENCE CHARACTERISTIC VELOCITY FOR HYPERBOLIC EXCESS REQUIREMENTS f_e = 0.42 to f_e = 0.50

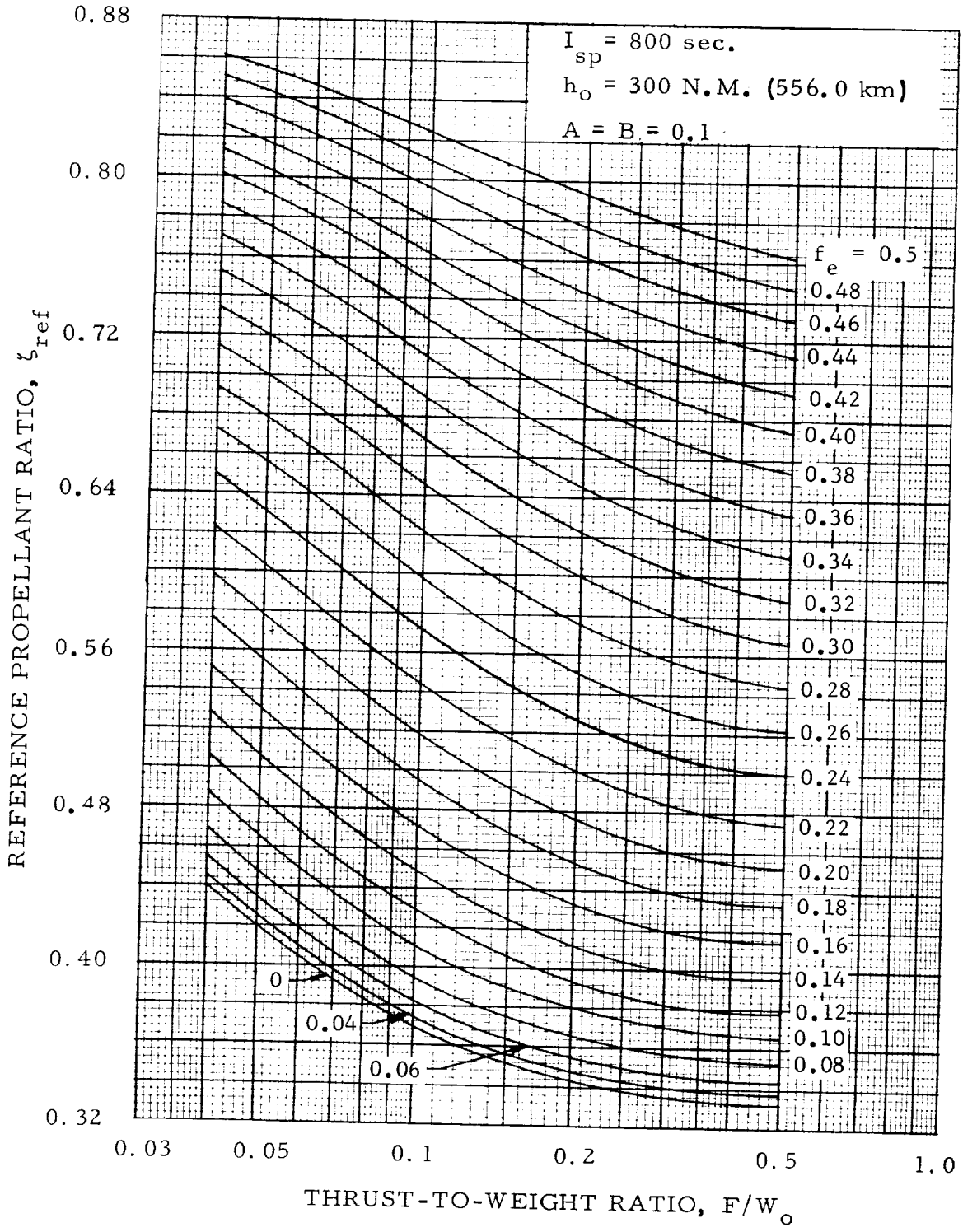

FIGURE 3. REFERENCE PROPELLANT RATIO FOR HYPERBOLIC EXCESS REQUIREMENTS

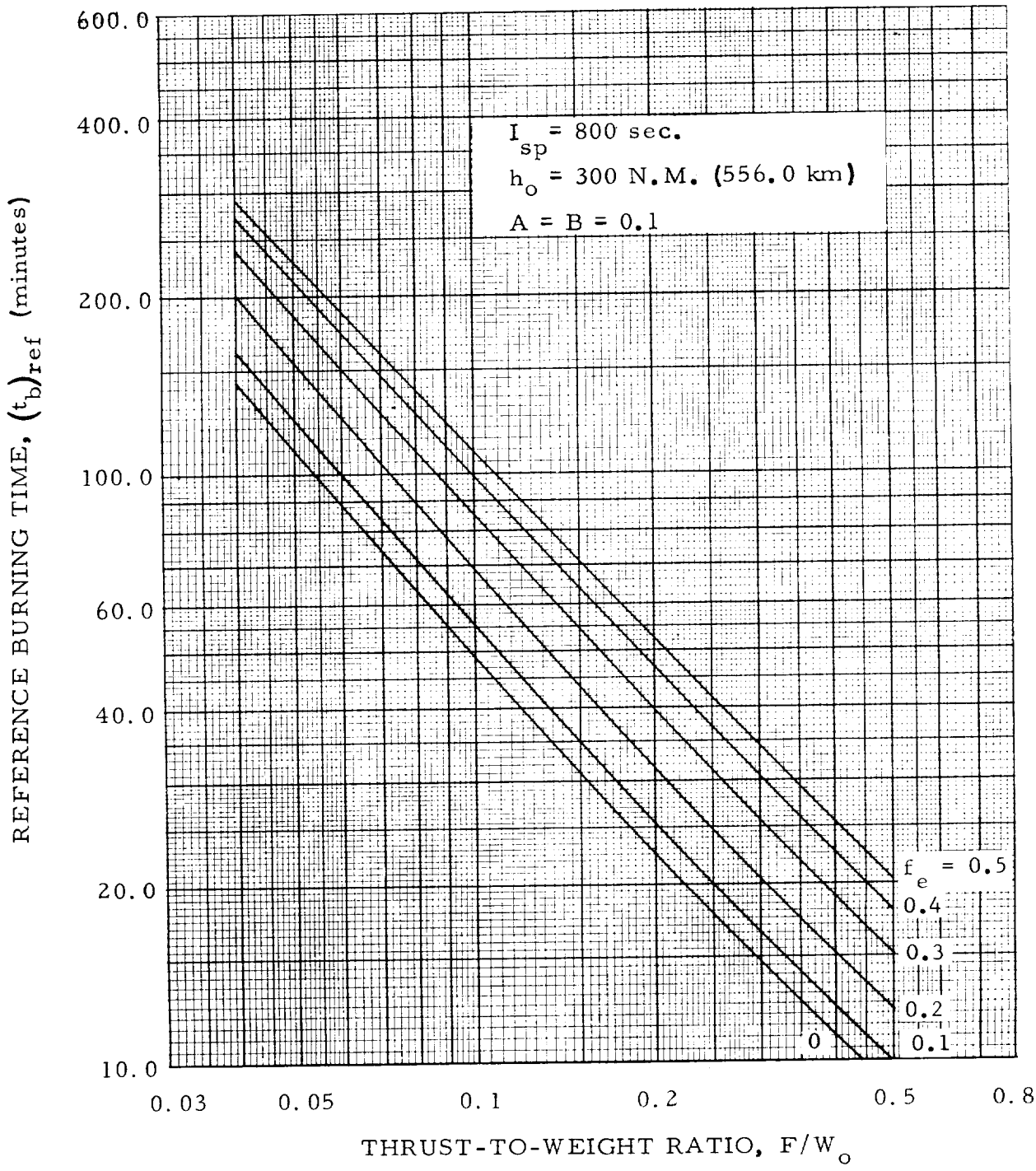

FIGURE 4. REFERENCE BURNING TIME AT INJECTION FOR HYPERBOLIC EXCESS REQUIREMENTS

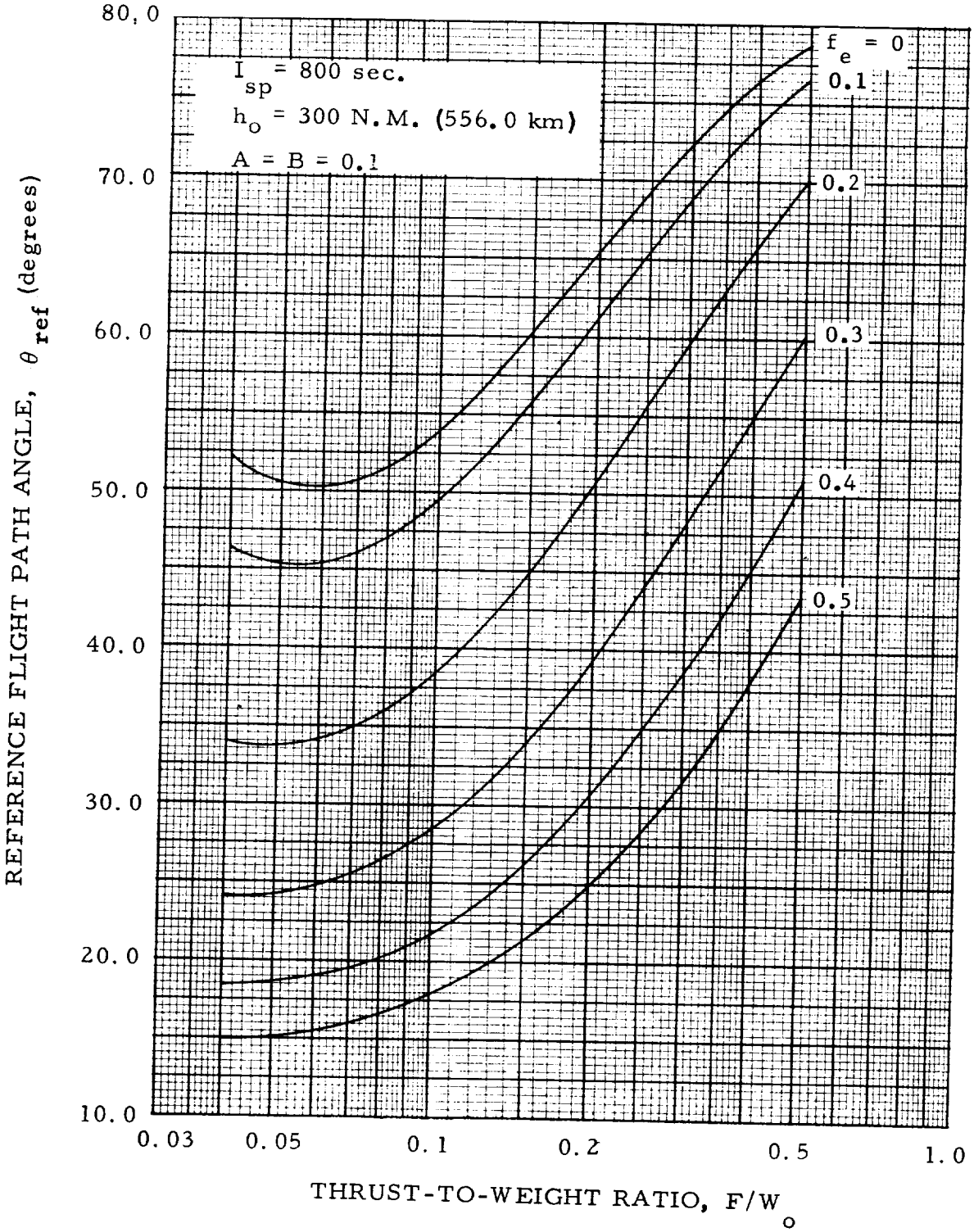

FIGURE 5. REFERENCE FLIGHT PATH ANGLE AT INJECTION FOR HYPERBOLIC EXCESS REQUIREMENTS

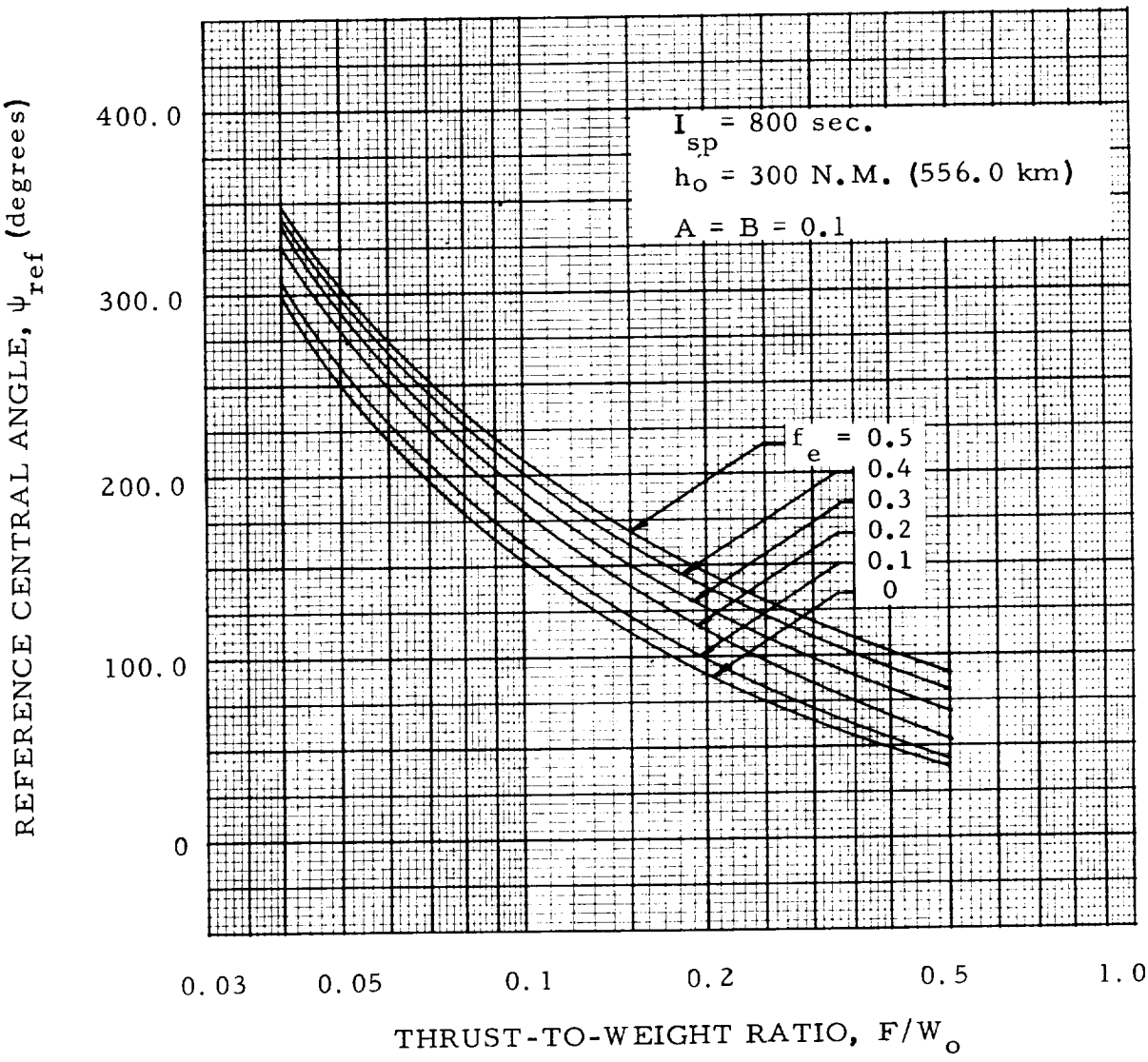

FIGURE 6. REFERENCE CENTRAL ANGLE AT INJECTION FOR HYPERBOLIC EXCESS REQUIREMENTS

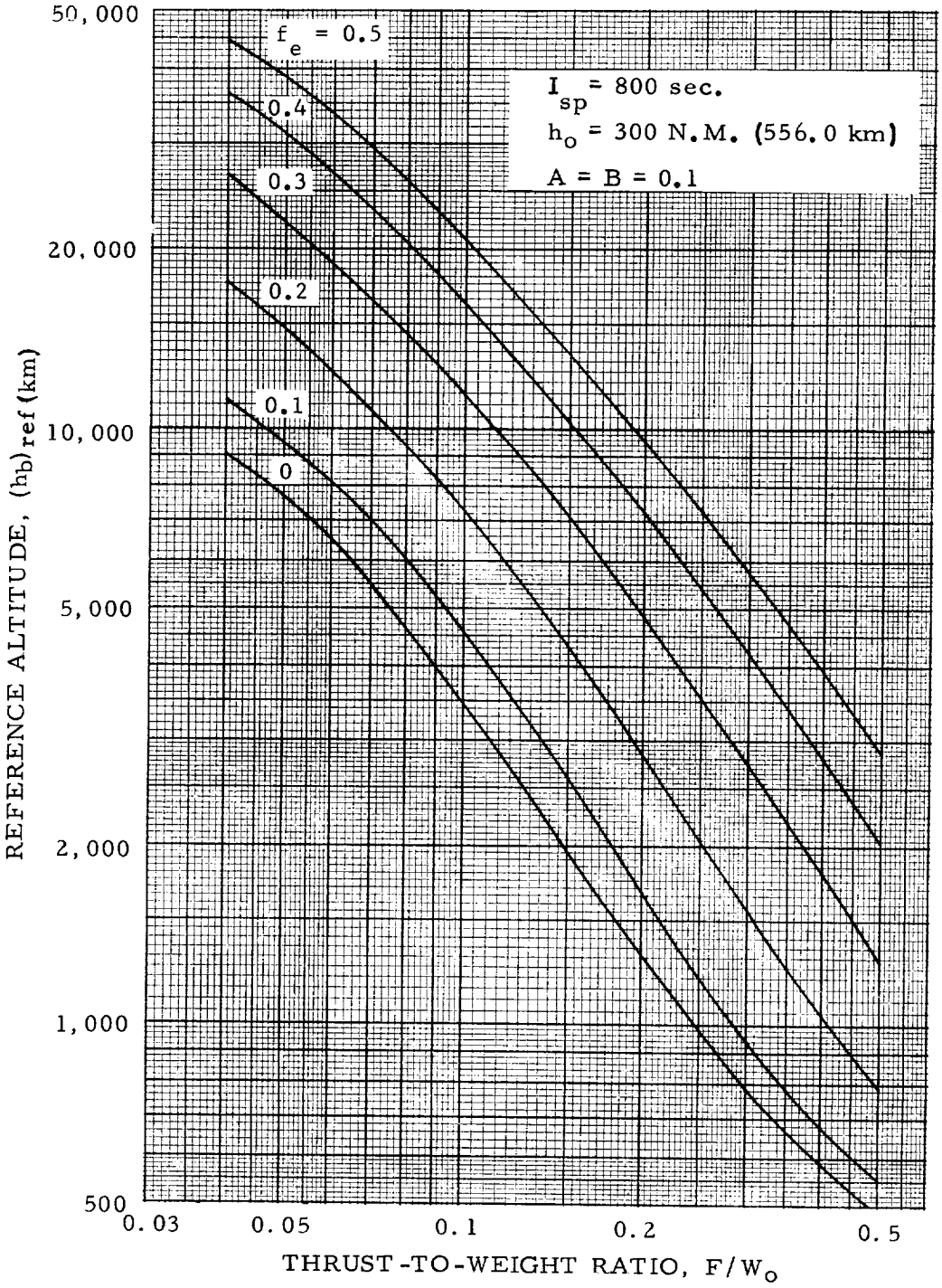

FIGURE 7. REFERENCE ALTITUDE AT INJECTION FOR HYPERBOLIC EXCESS REQUIREMENTS

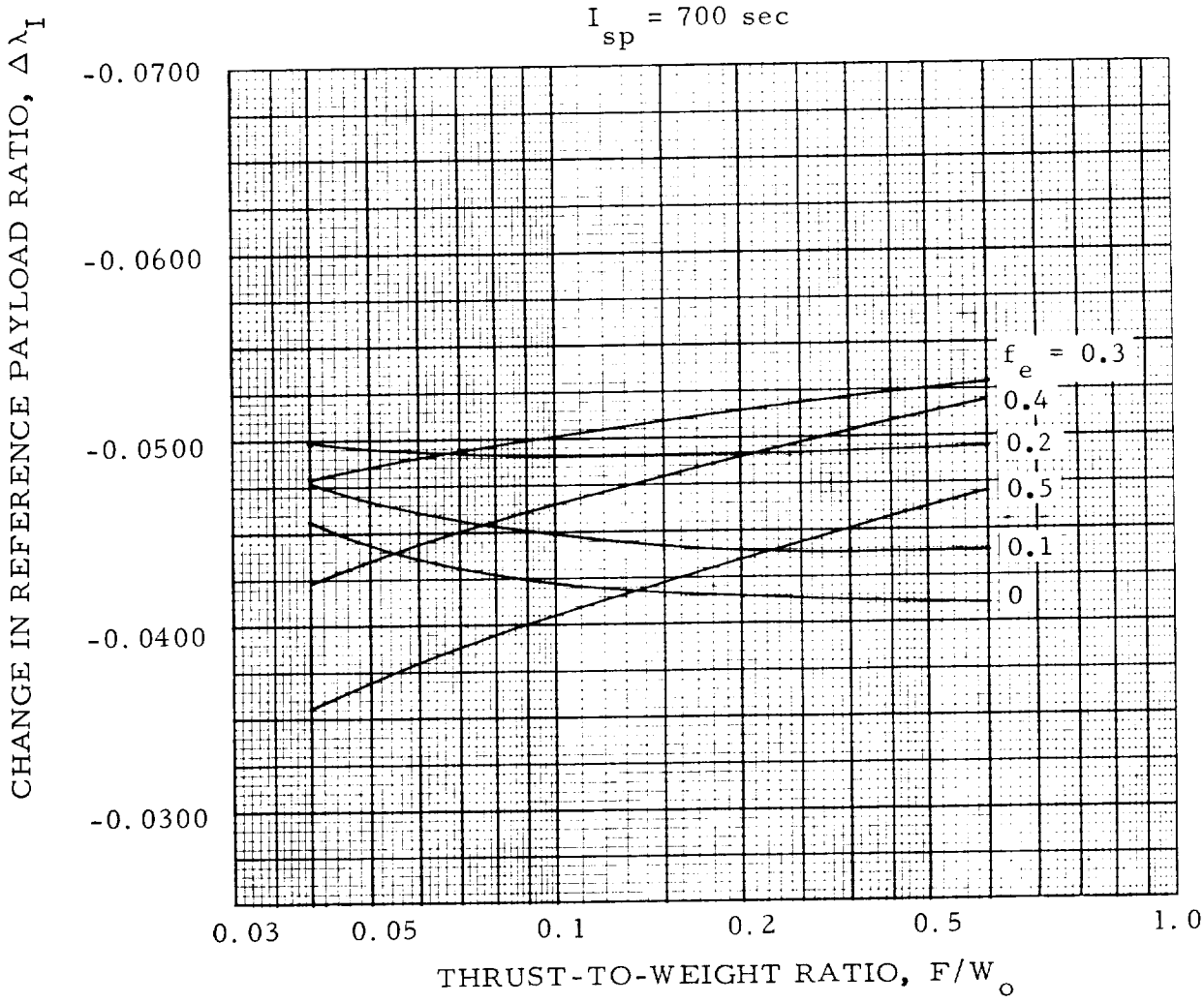

FIGURE 8a. CHANGE IN REFERENCE PAYLOAD RATIO FOR NON-REFERENCE SPECIFIC IMPULSES

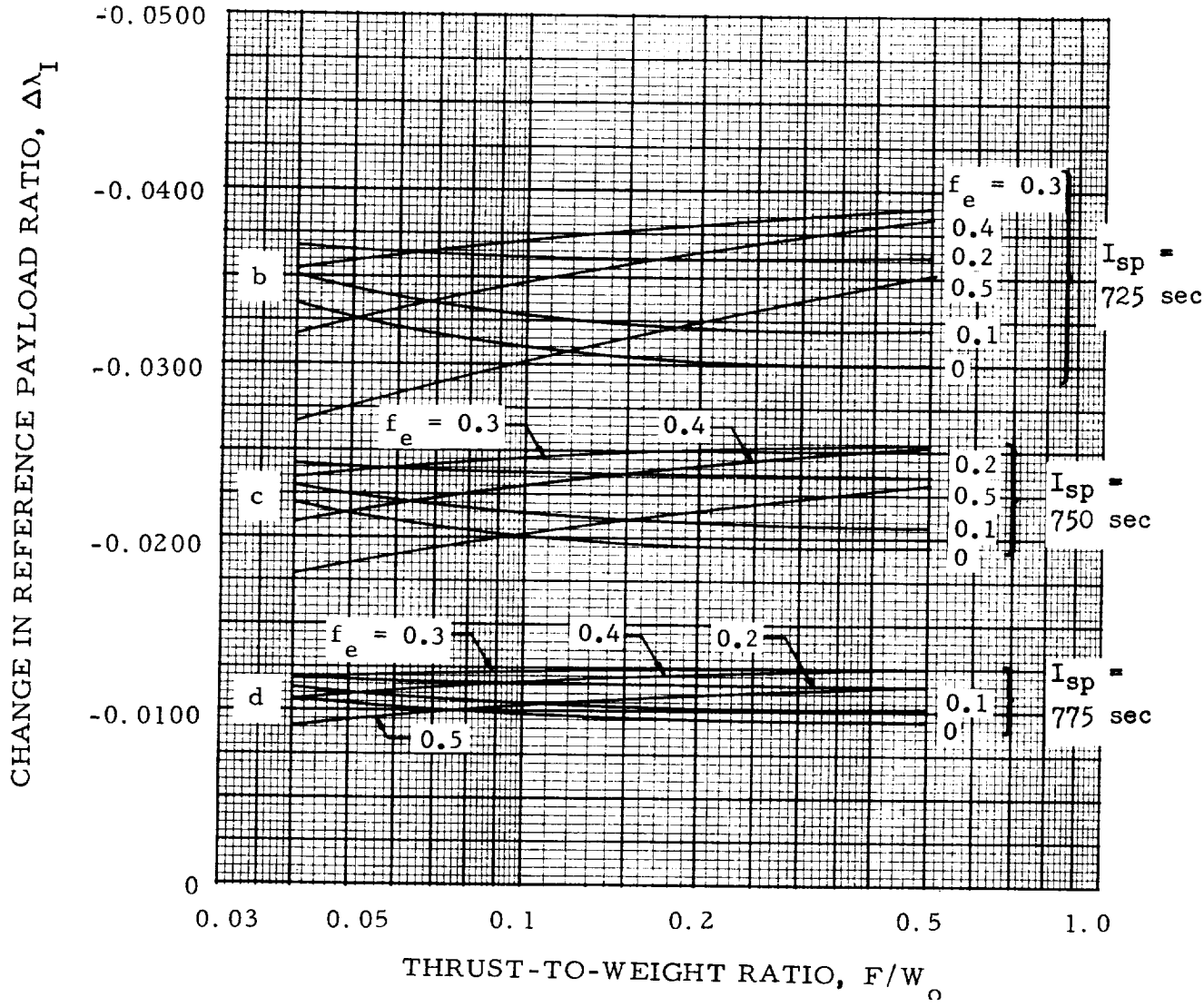

FIGURE 8b, c, d. CHANGE IN REFERENCE PAYLOAD RATIO FOR NON-REFERENCE SPECIFIC IMPULSES

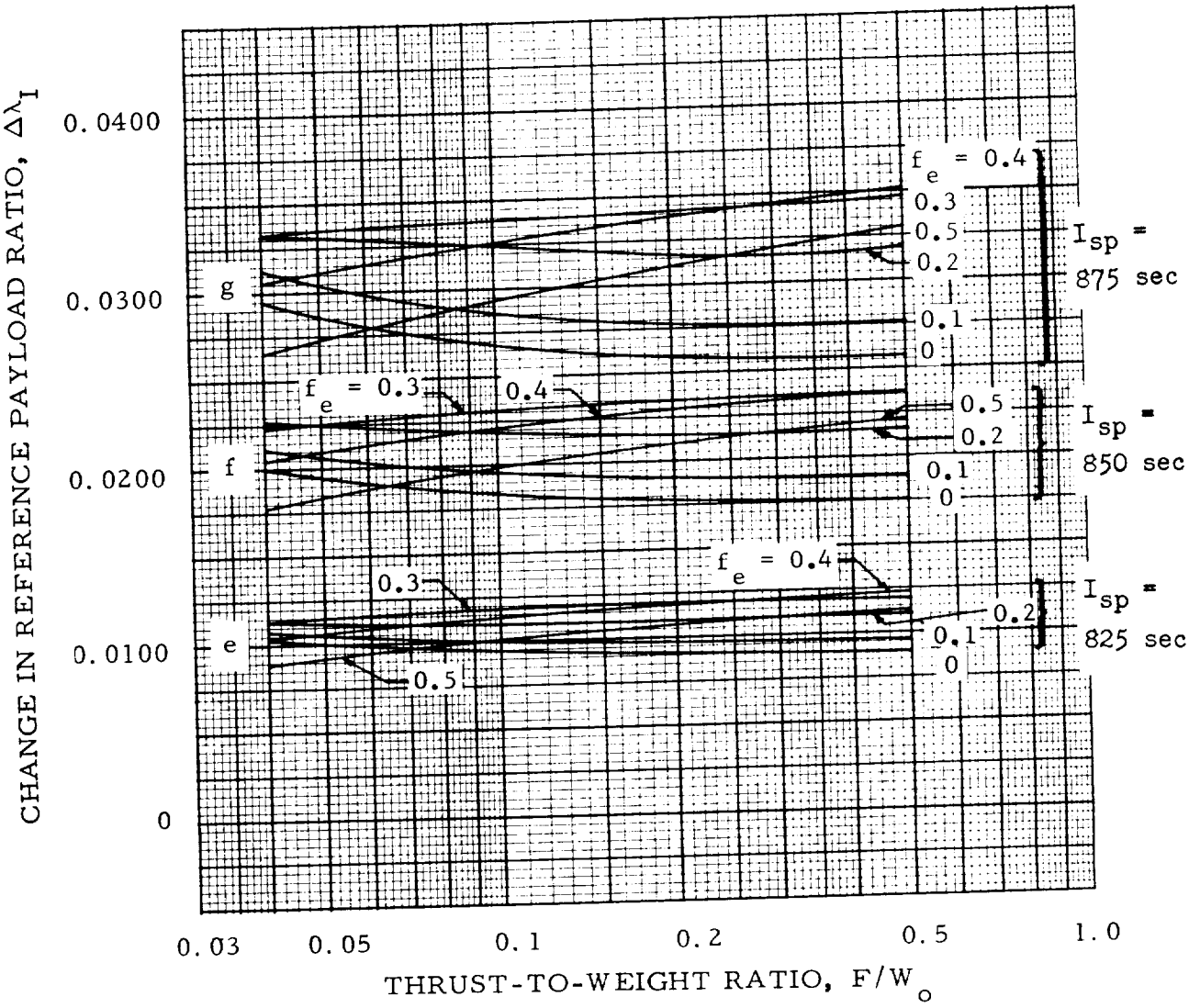

FIGURE 8e, f, g. CHANGE IN REFERENCE PAYLOAD RATIO FOR NON-REFERENCE SPECIFIC IMPULSES

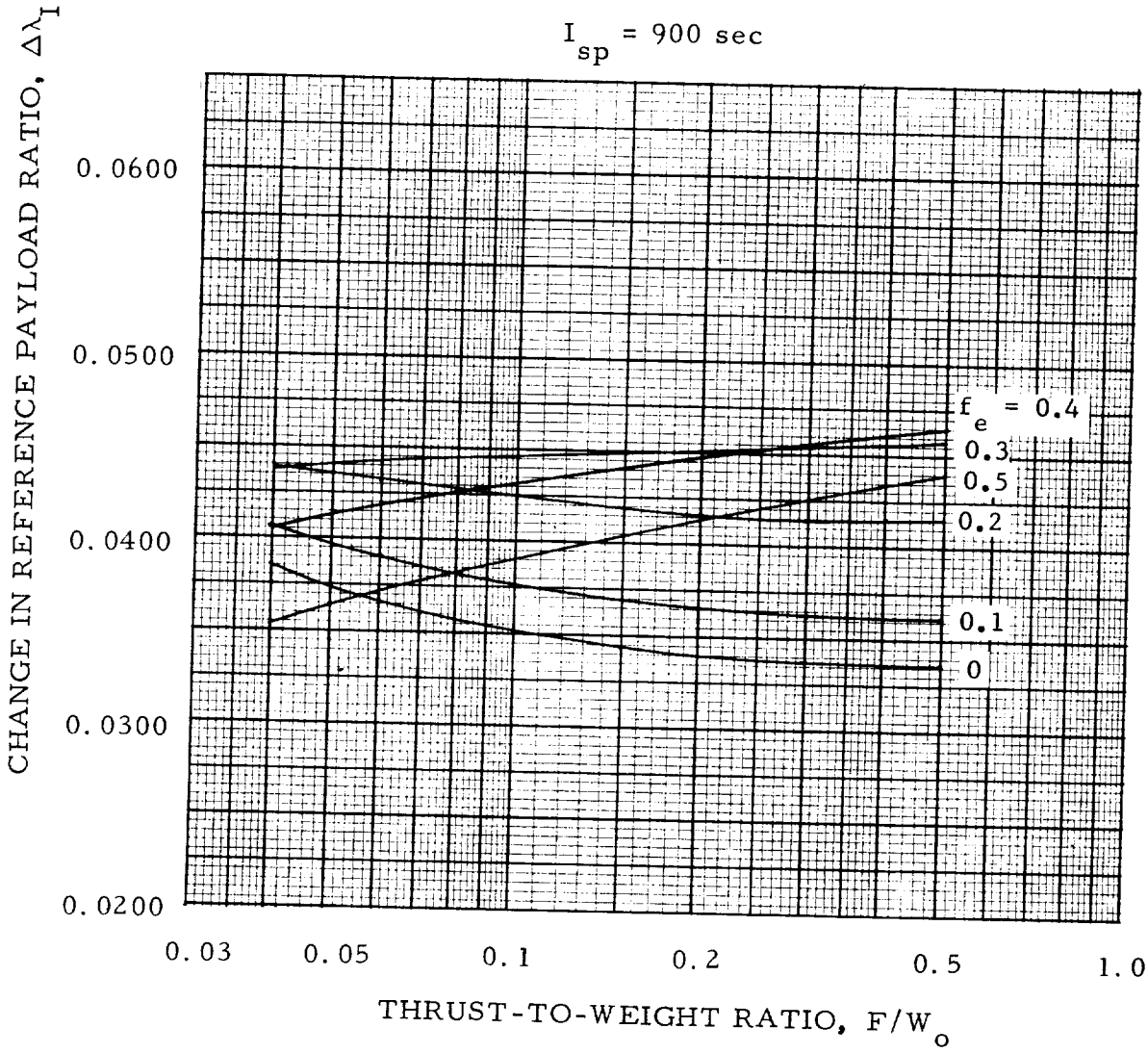

FIGURE 8h. CHANGE IN REFERENCE PAYLOAD RATIO FOR NON-REFERENCE SPECIFIC IMPULSES

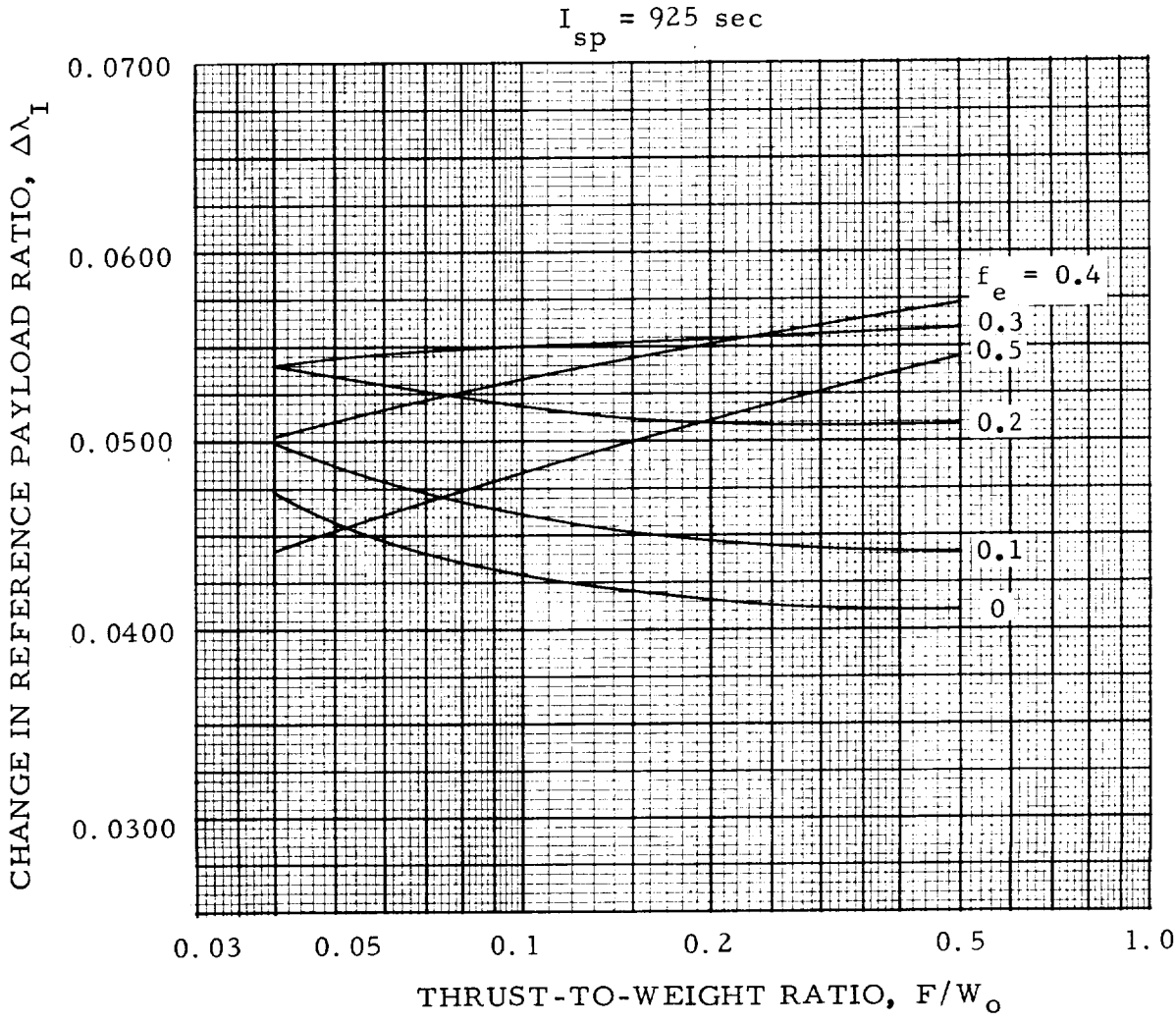

FIGURE 8i. CHANGE IN REFERENCE PAYLOAD RATIO FOR NON-REFERENCE SPECIFIC IMPULSES

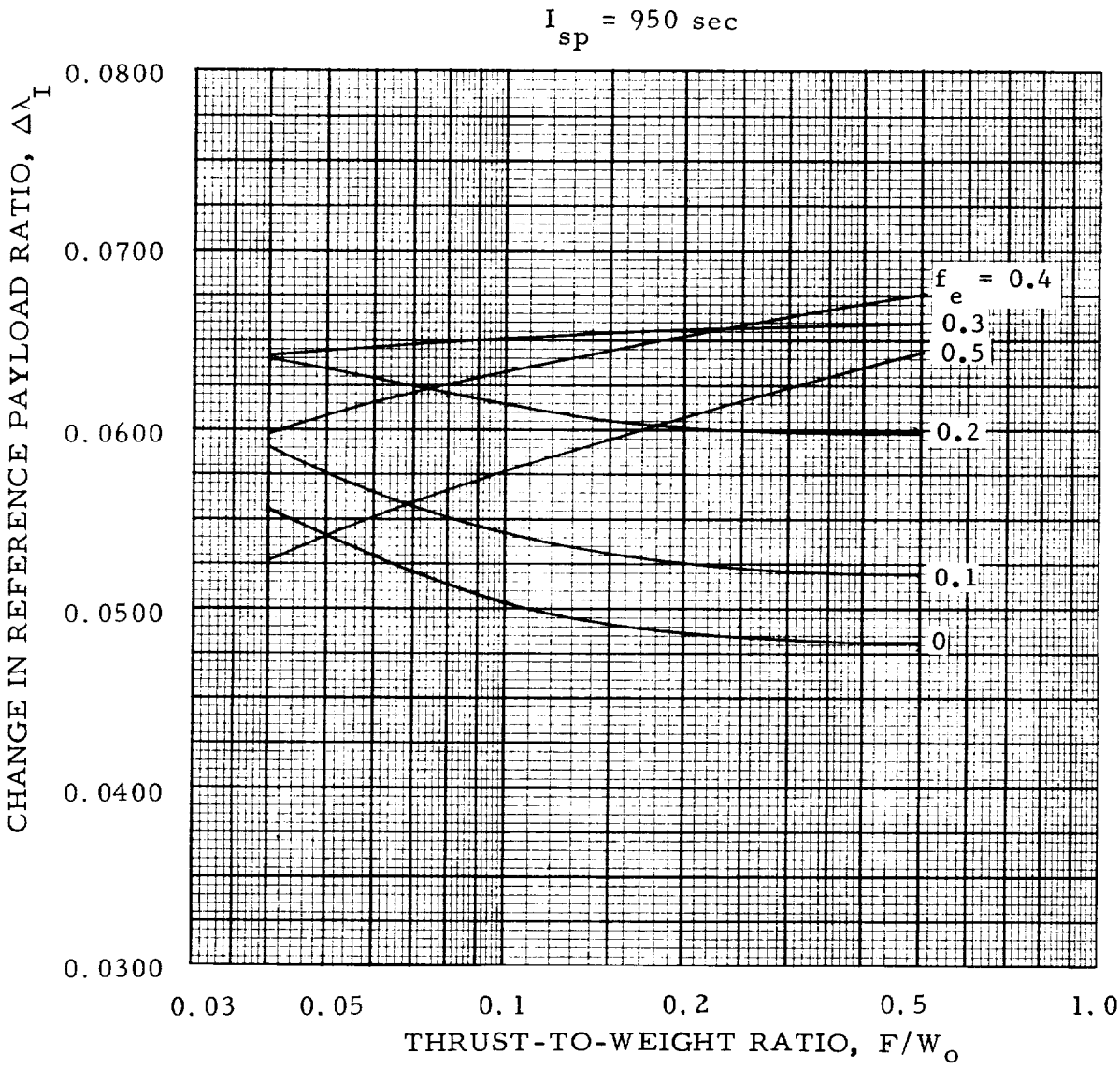

FIGURE 8j. CHANGE IN REFERENCE PAYLOAD RATIO FOR NON-REFERENCE SPECIFIC IMPULSES

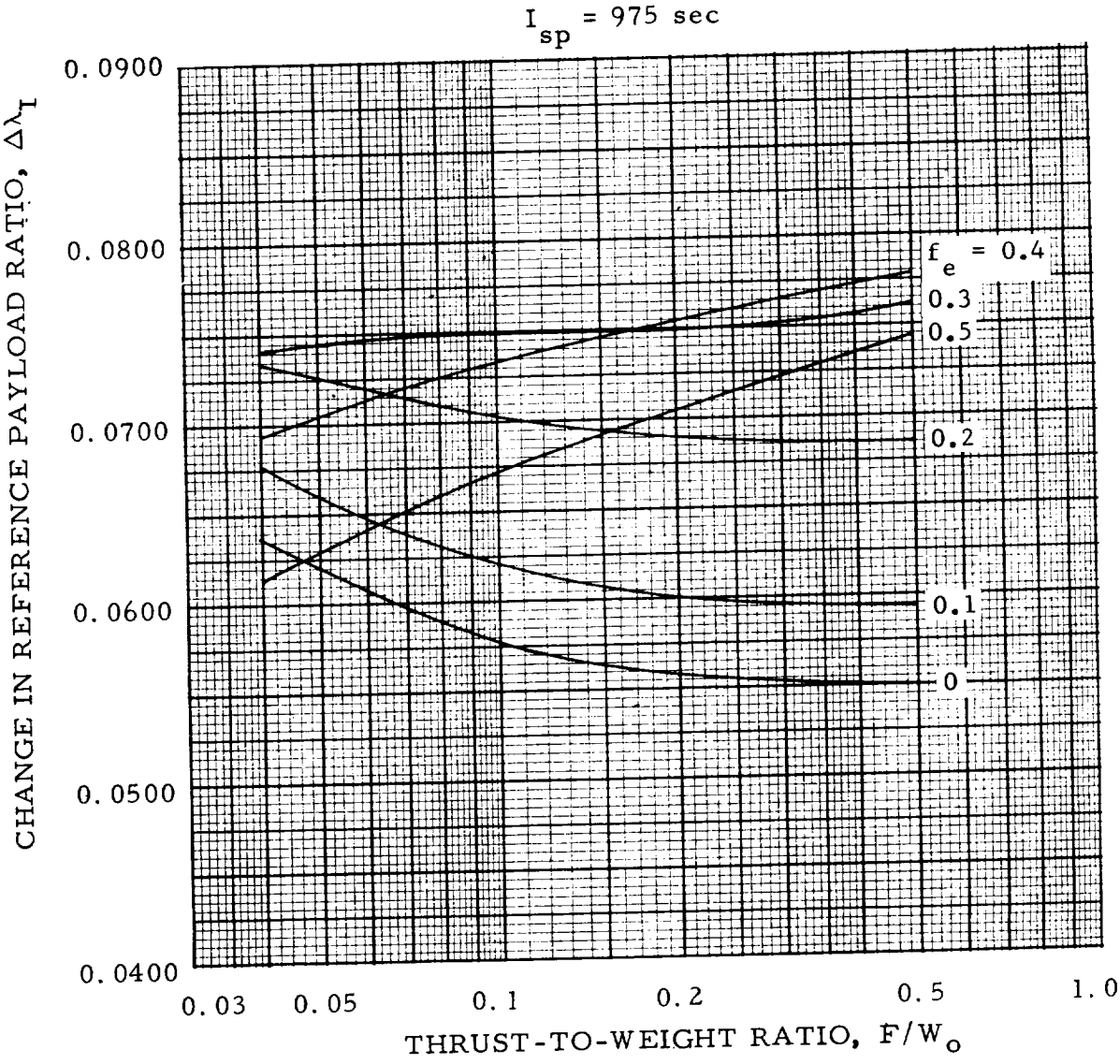

FIGURE 8k. CHANGE IN REFERENCE PAYLOAD RATIO FOR NON-REFERENCE SPECIFIC IMPULSES

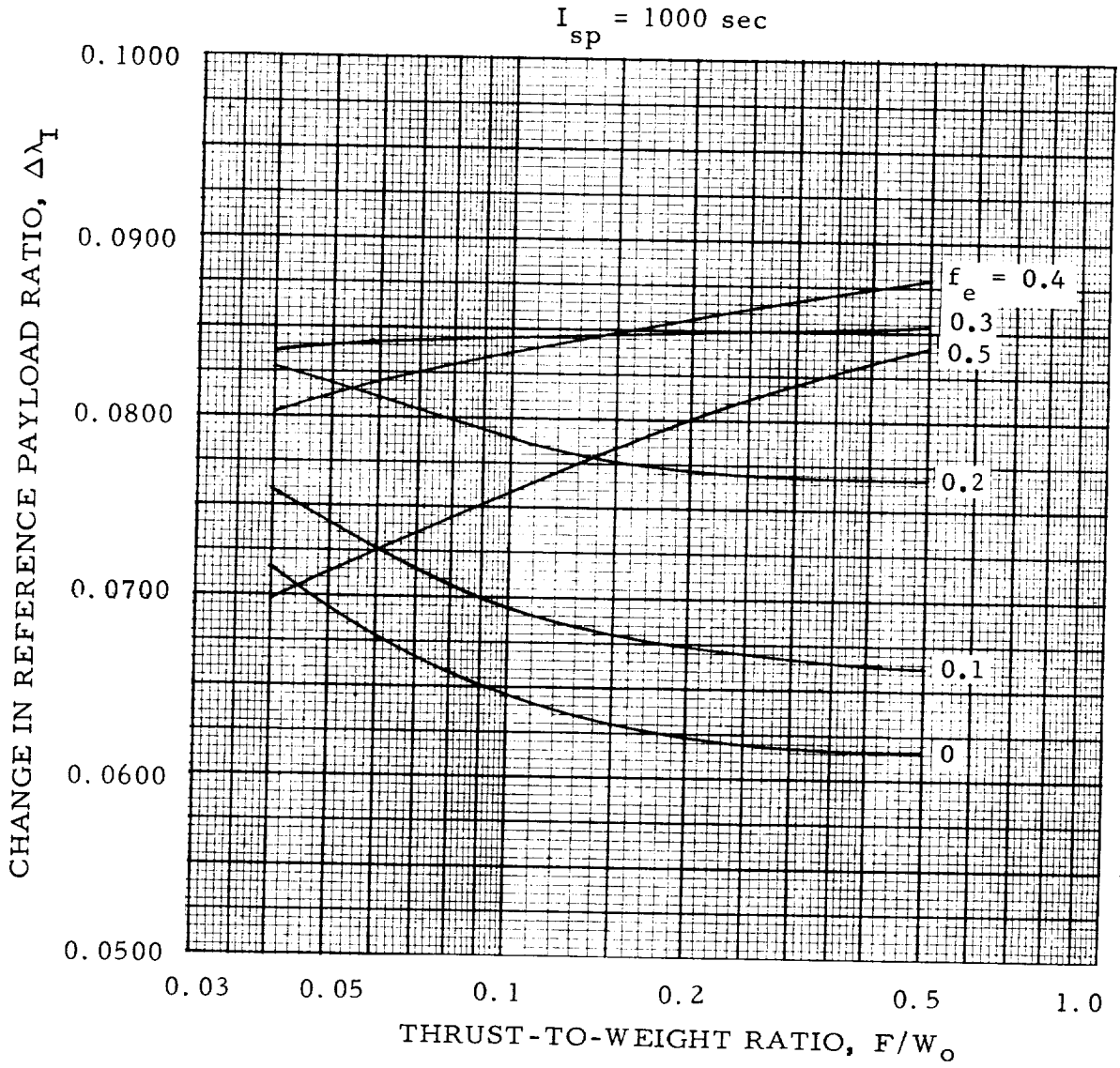

FIGURE 8ℓ. CHANGE IN REFERENCE PAYLOAD RATIO FOR NON-REFERENCE SPECIFIC IMPULSES

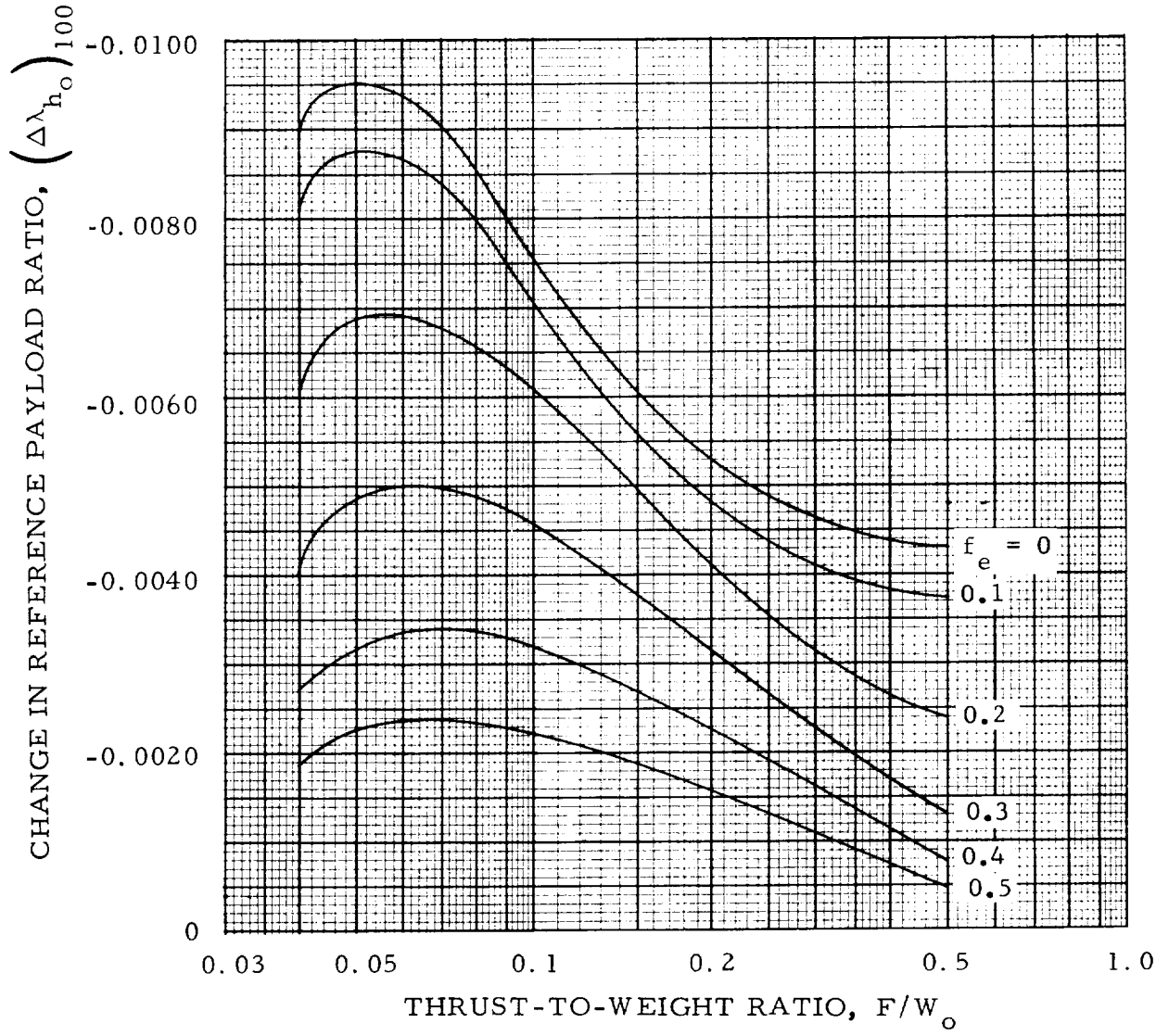

FIGURE 9. CHANGE IN REFERENCE PAYLOAD RATIO FOR INCREMENTAL ALTITUDE DECREASE OF 100 N. M.

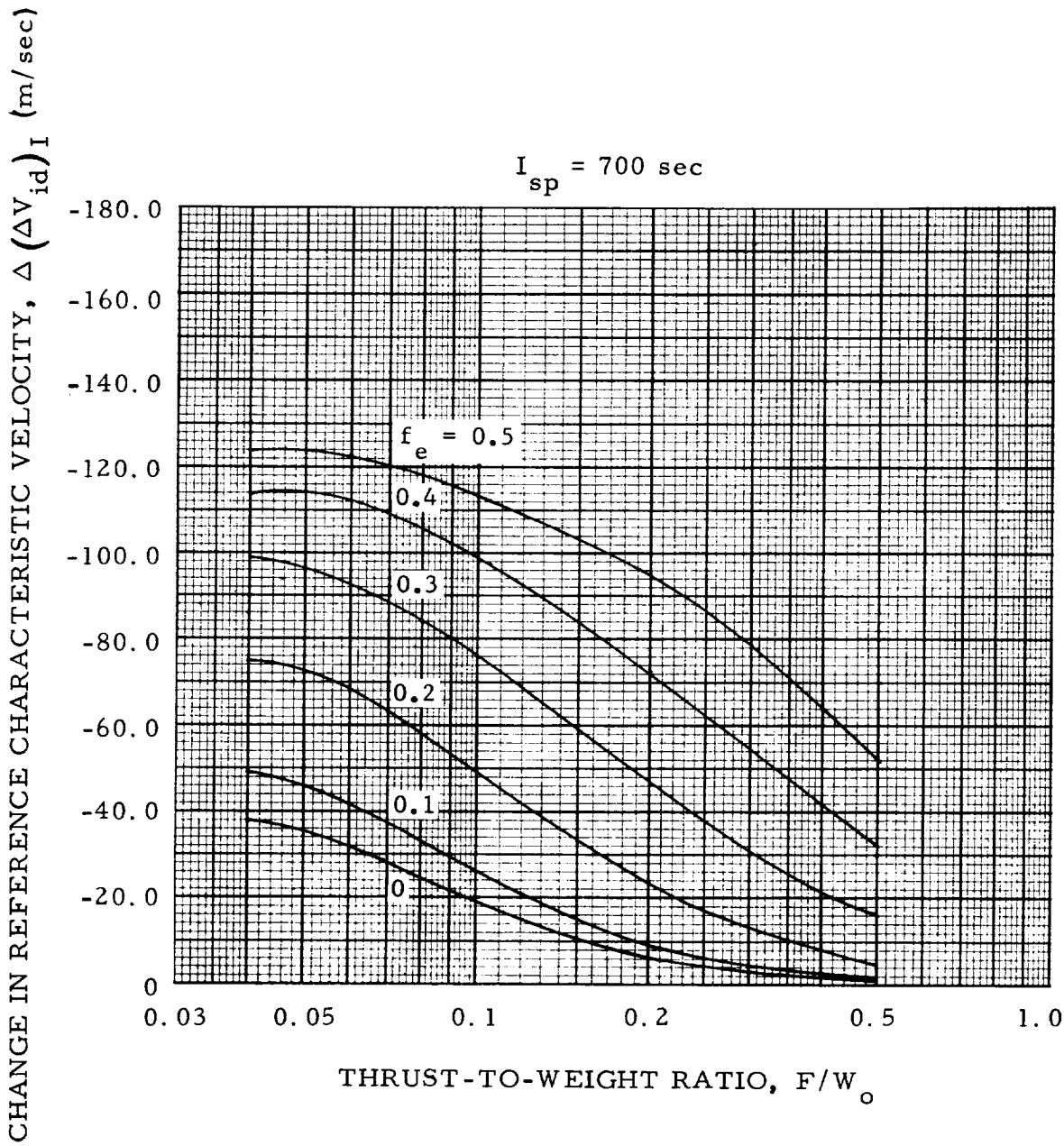

FIGURE 10a. CHANGE IN REFERENCE CHARACTERISTIC VELOCITY FOR NON-REFERENCE SPECIFIC IMPULSES

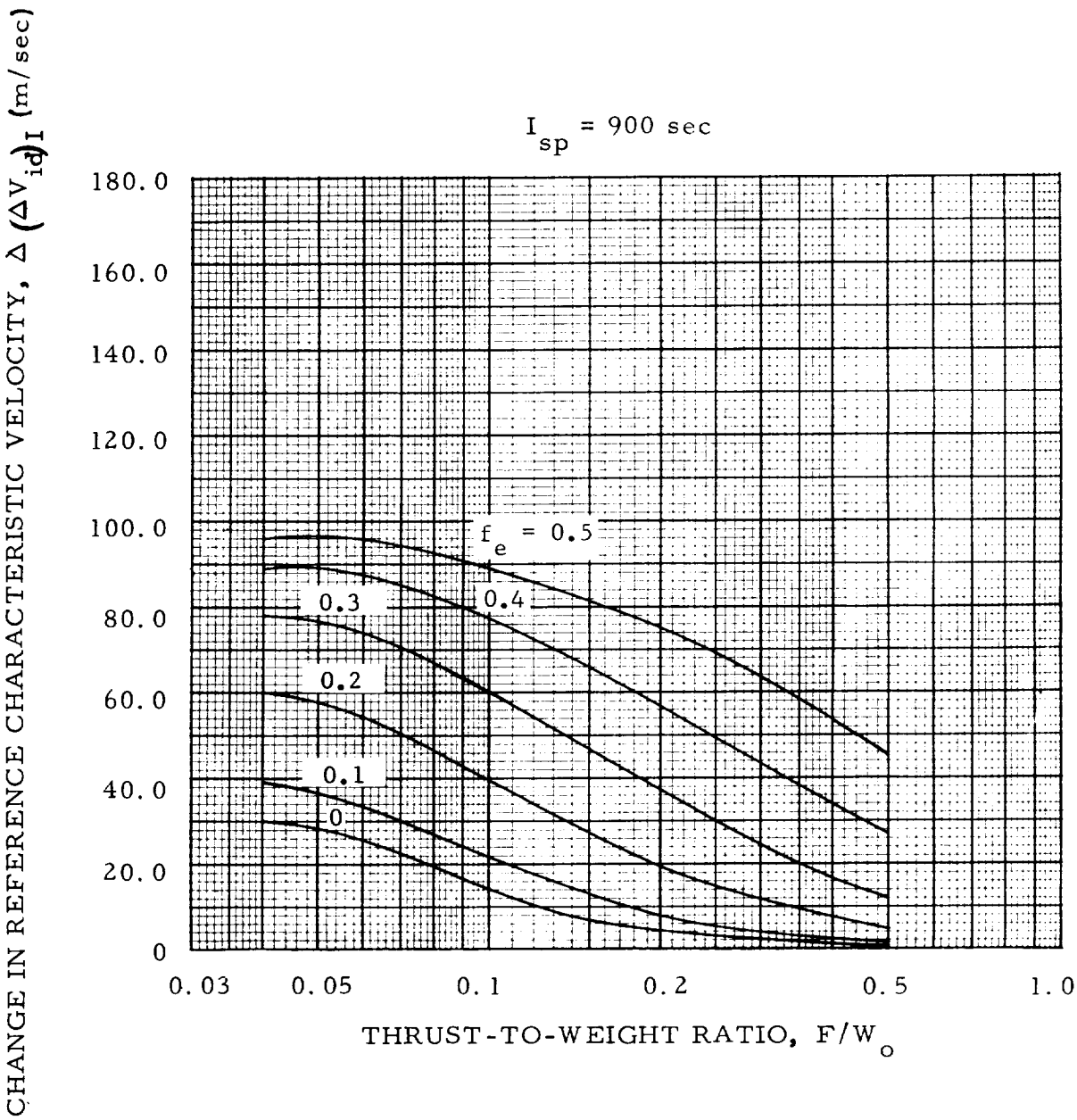

FIGURE 10b. CHANGE IN REFERENCE CHARACTERISTIC VELOCITY FOR NON-REFERENCE SPECIFIC IMPULSE

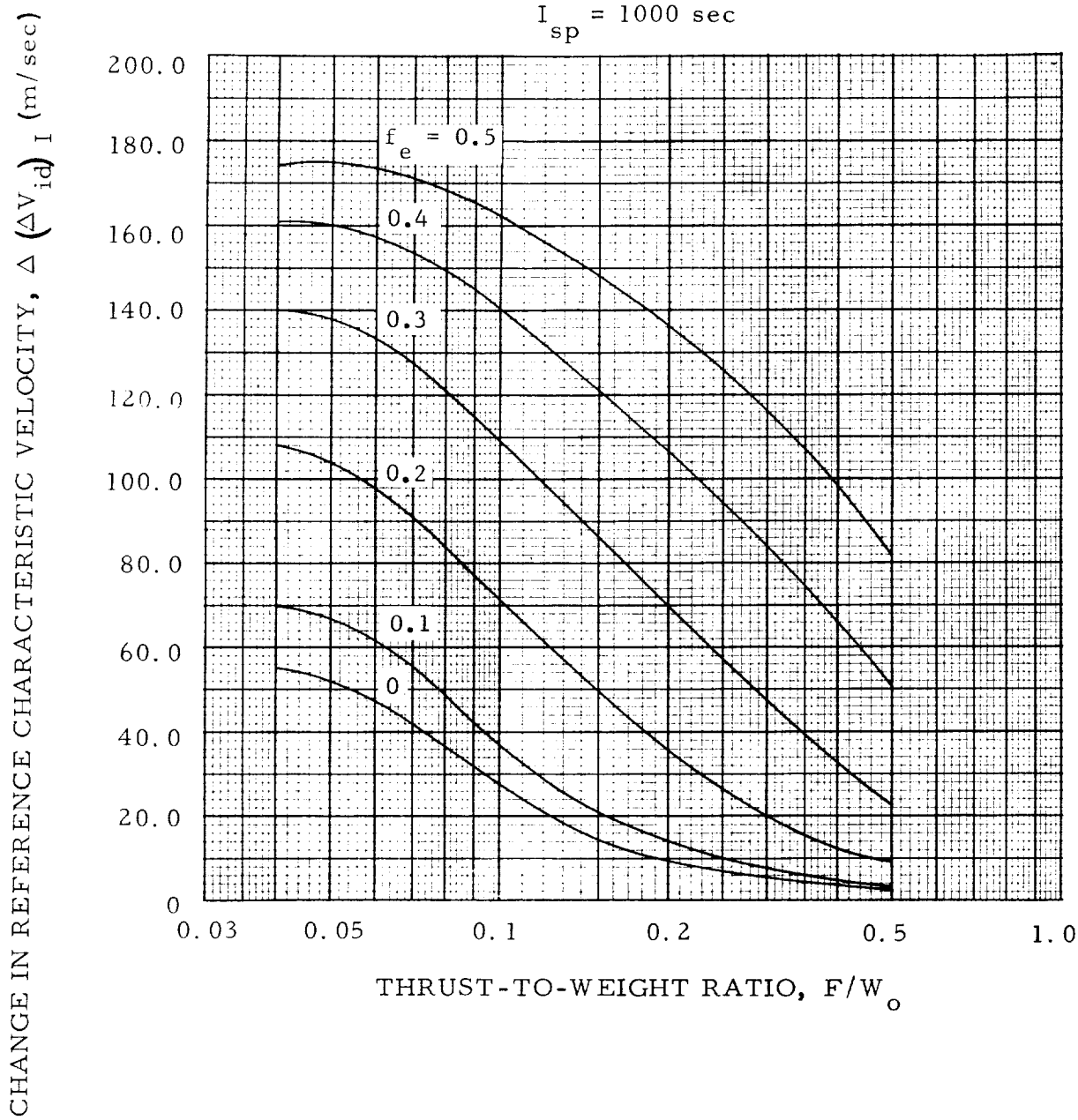

FIGURE 10c. CHANGE IN REFERENCE CHARACTERISTIC VELOCITY FOR NON-REFERENCE SPECIFIC IMPULSE

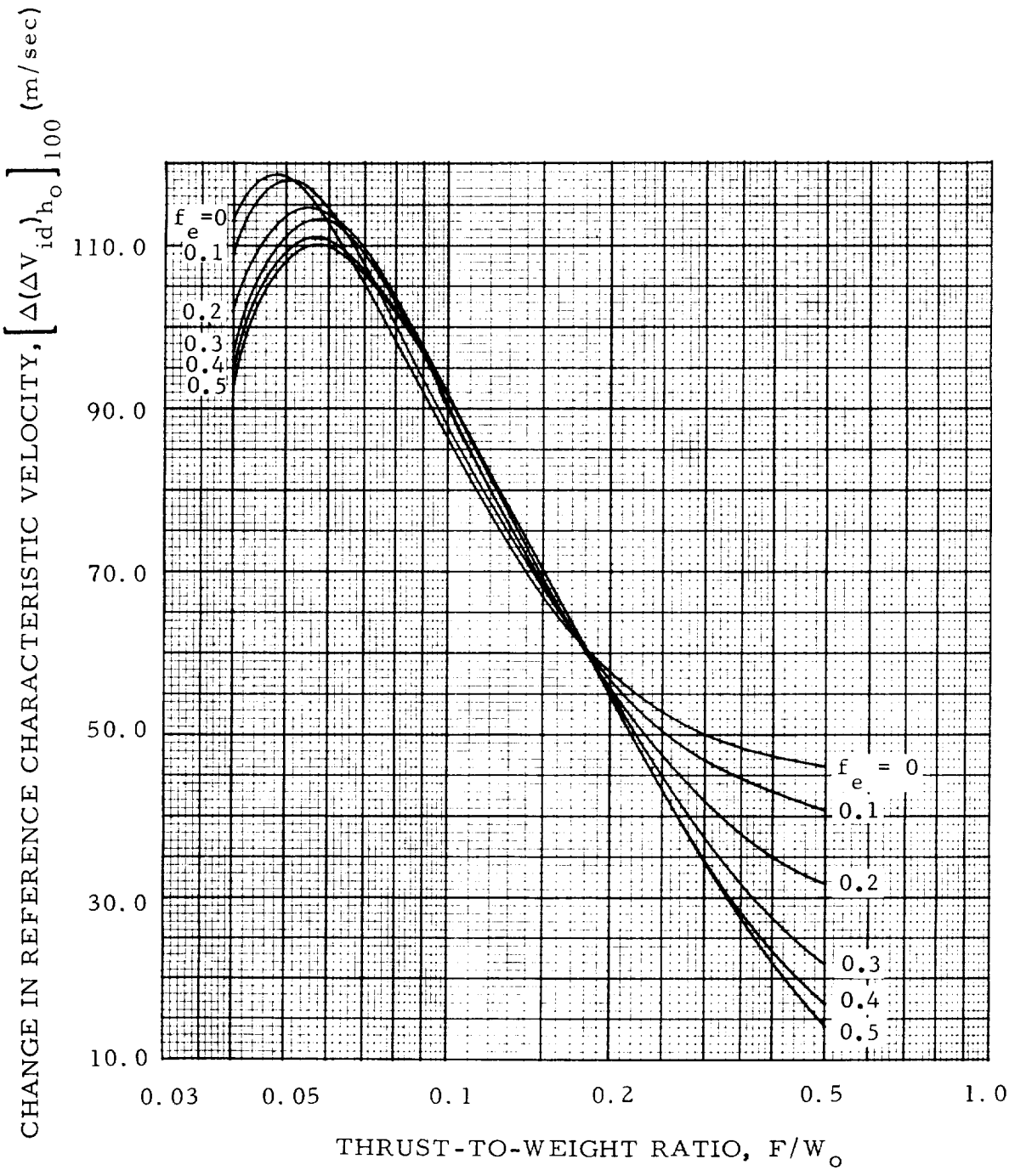

FIGURE 11. CHANGE IN REFERENCE CHARACTERISTIC VELOCITY FOR INCREMENTAL ALTITUDE DECREASE OF 100 N.M.

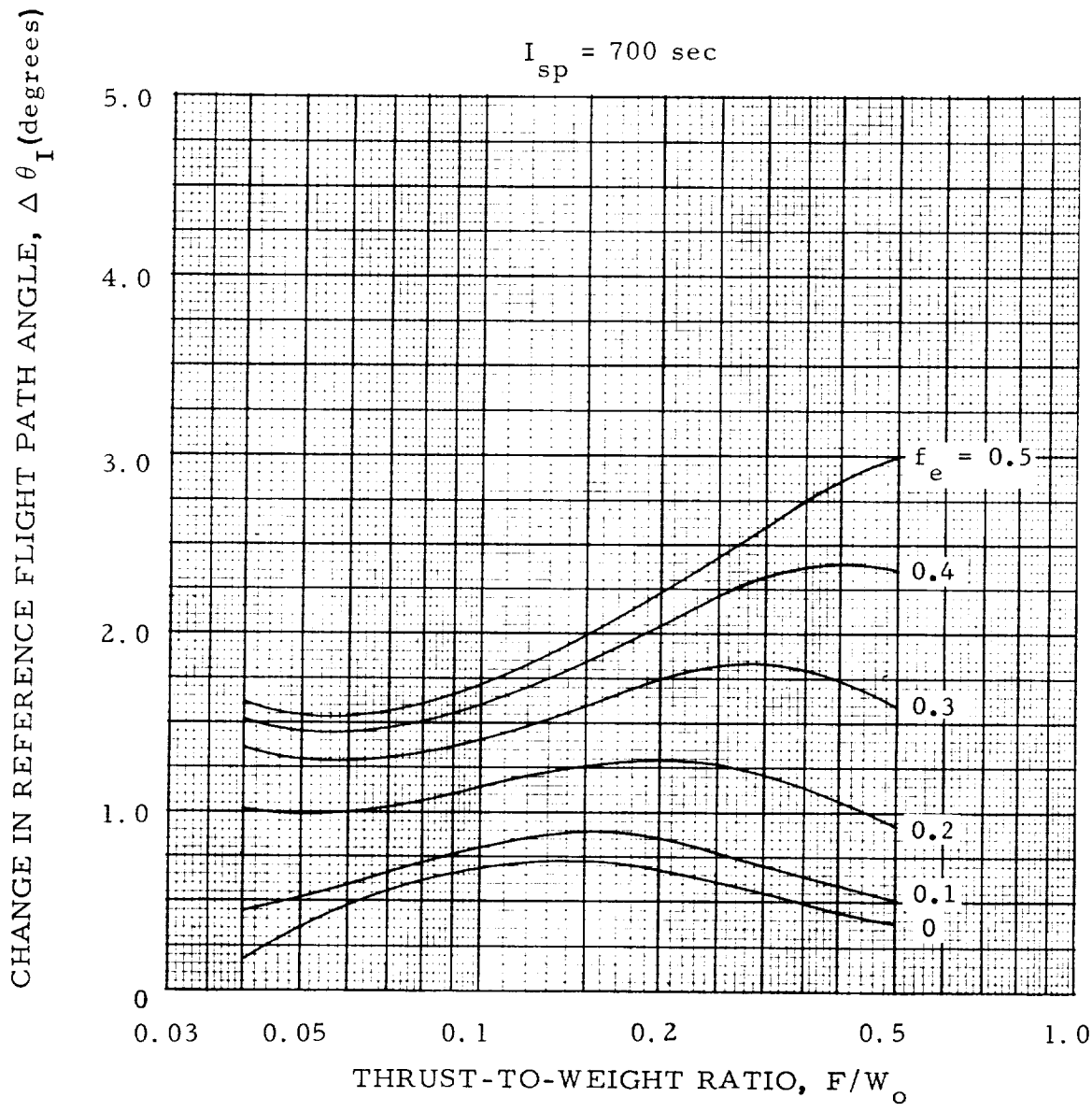

FIGURE 12a. CHANGE IN REFERENCE FLIGHT PATH ANGLE AT INJECTION FOR NON-REFERENCE SPECIFIC IMPULSES

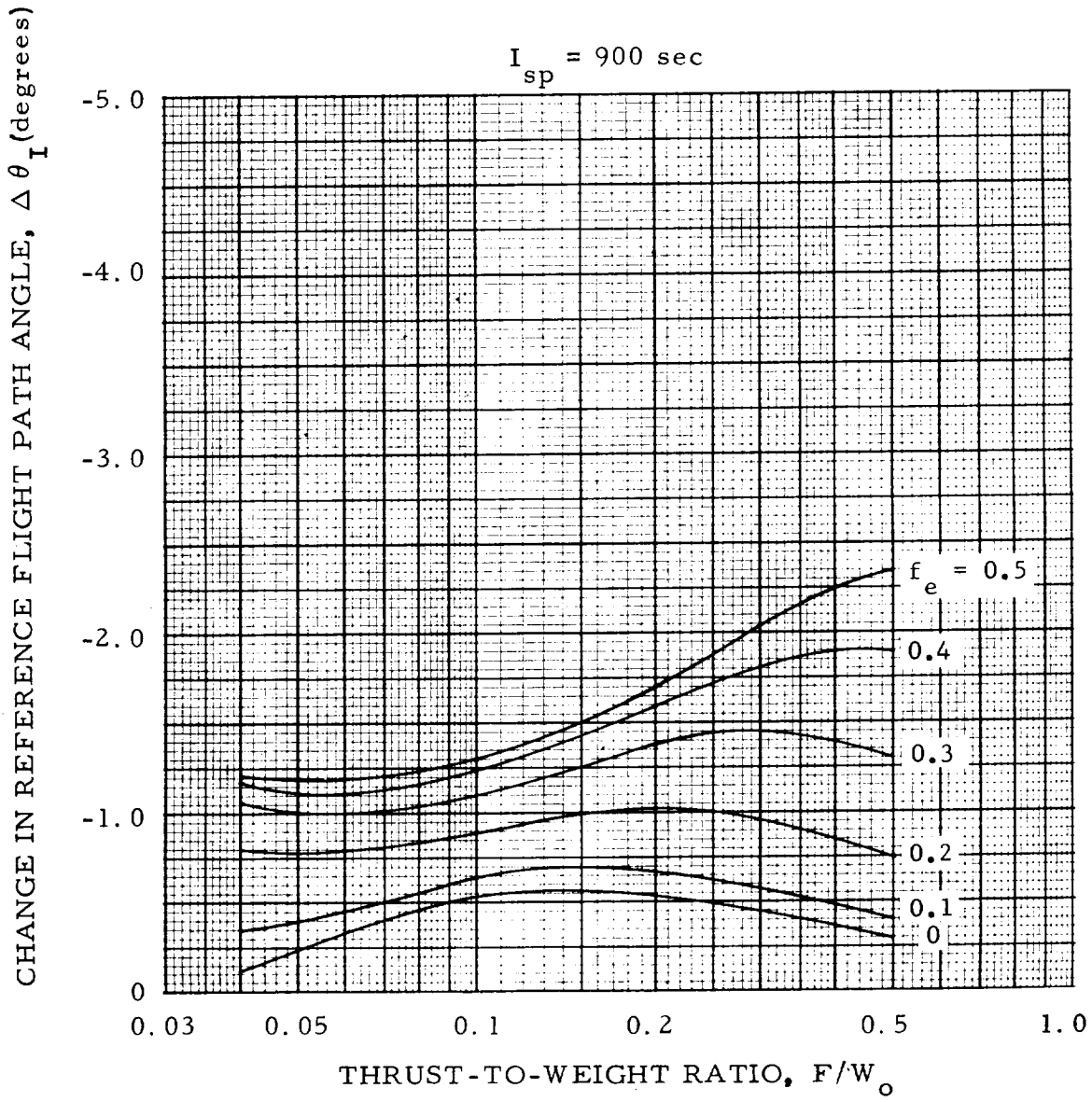

FIGURE 12b. CHANGE IN REFERENCE FLIGHT PATH ANGLE AT INJECTION FOR NON-REFERENCE SPECIFIC IMPULSES

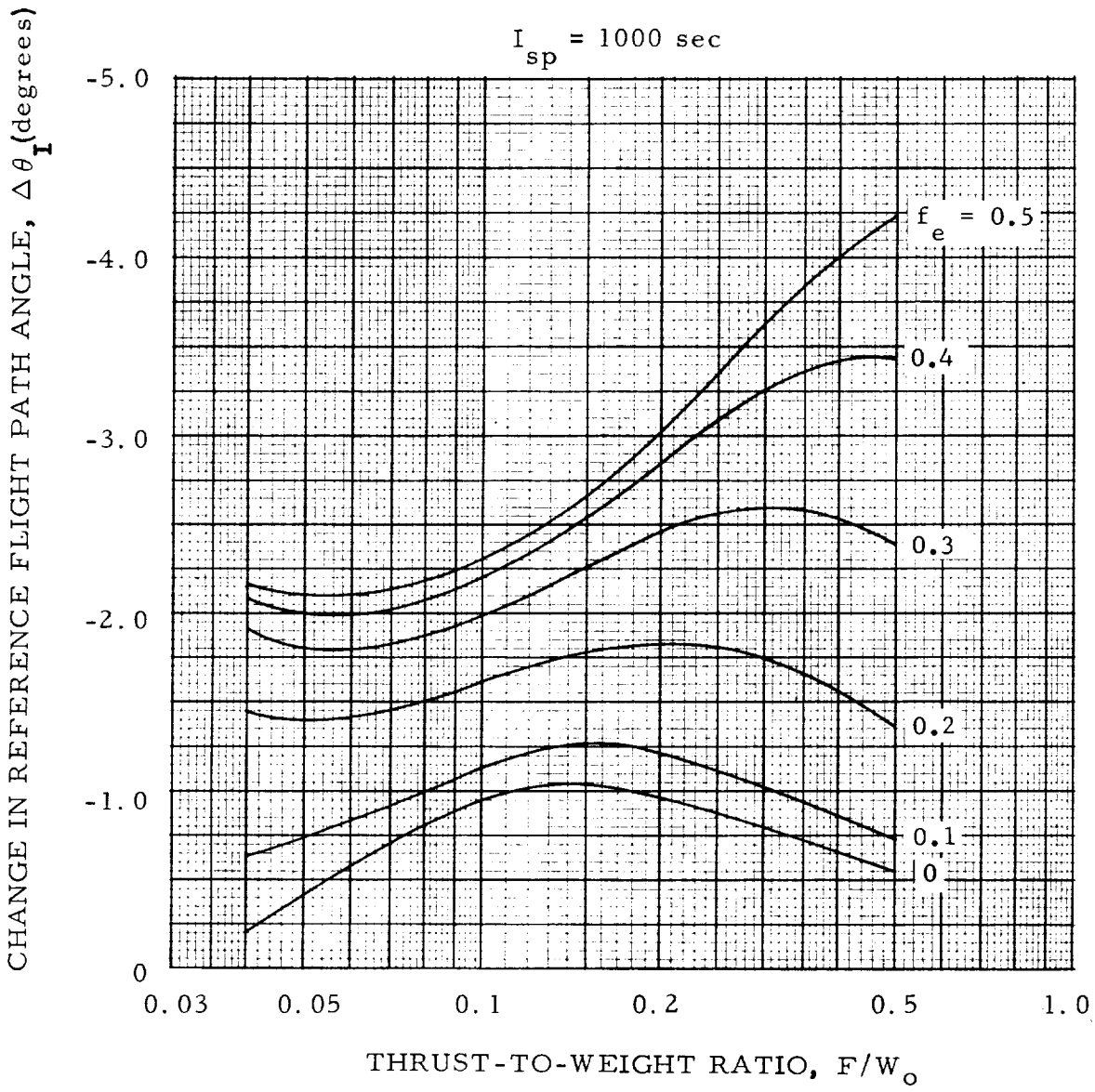

FIGURE 12c. CHANGE IN REFERENCE FLIGHT PATH ANGLE AT INJECTION FOR NON-REFERENCE SPECIFIC IMPULSES

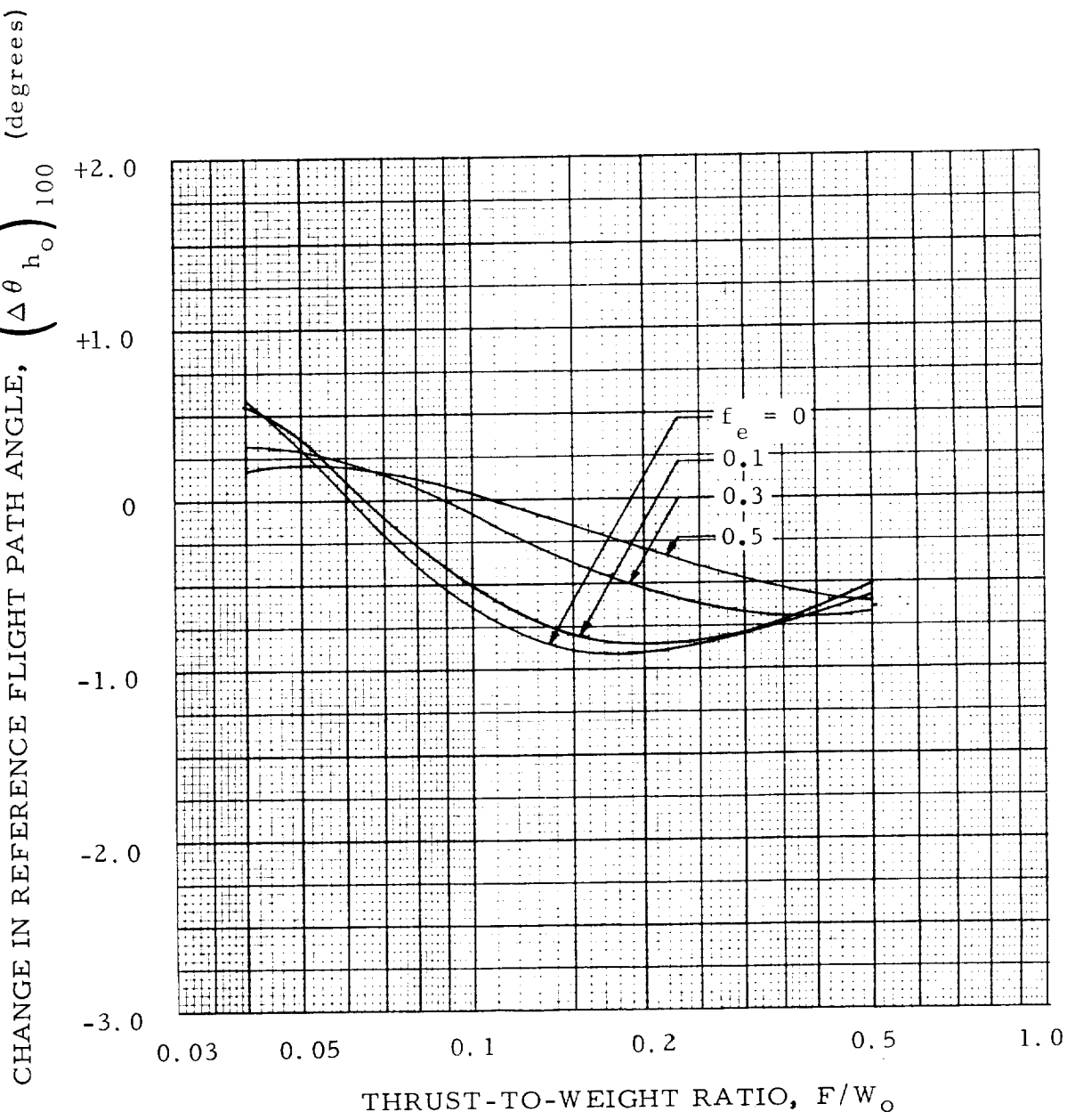

FIGURE 13. CHANGE IN REFERENCE FLIGHT PATH ANGLE AT INJECTION FOR INCREMENTAL ALTITUDE DECREASE OF 100 N. M.

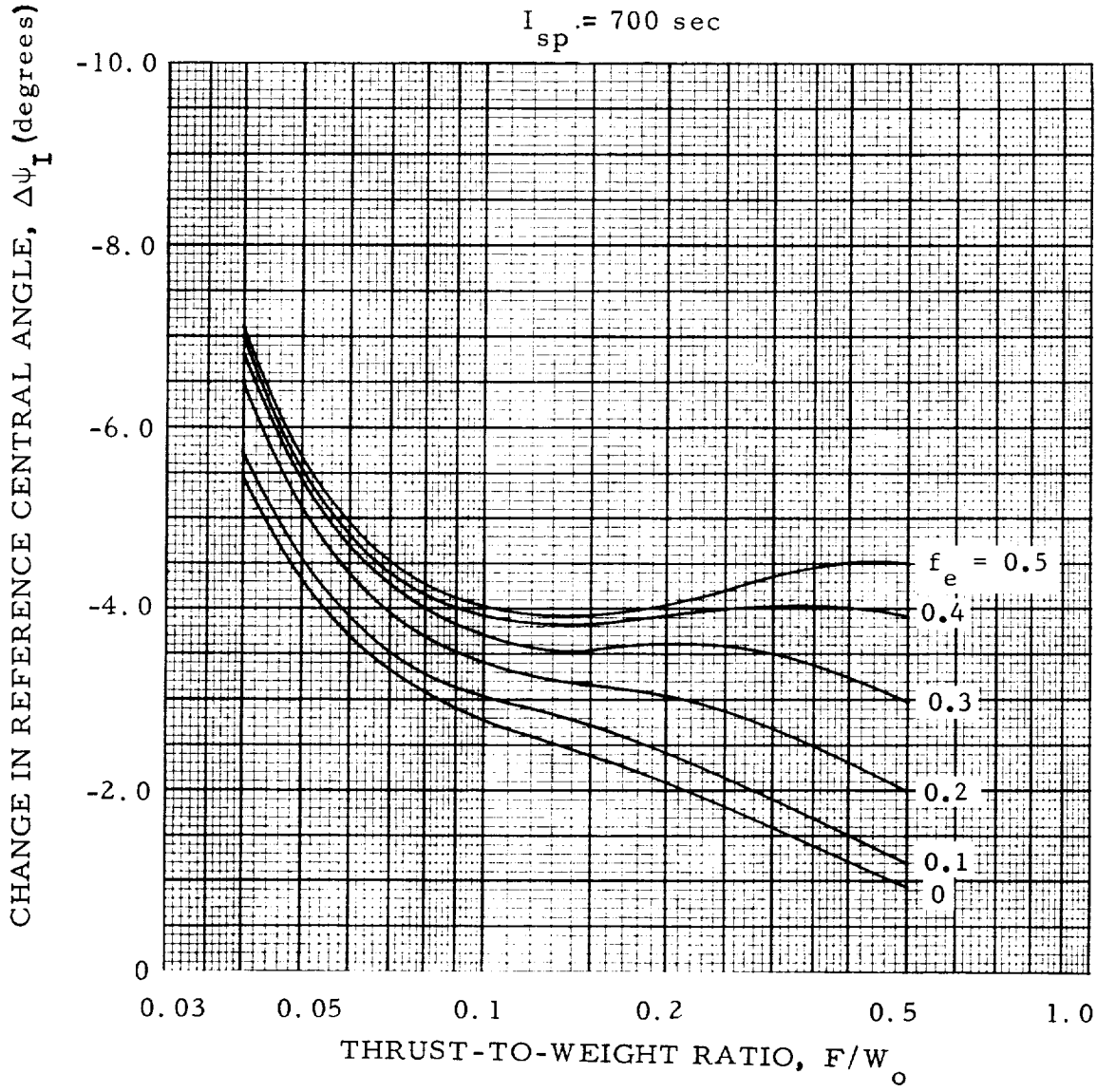

FIGURE 14a. CHANGE IN REFERENCE CENTRAL ANGLE AT INJECTION FOR NON-REFERENCE SPECIFIC IMPULSES

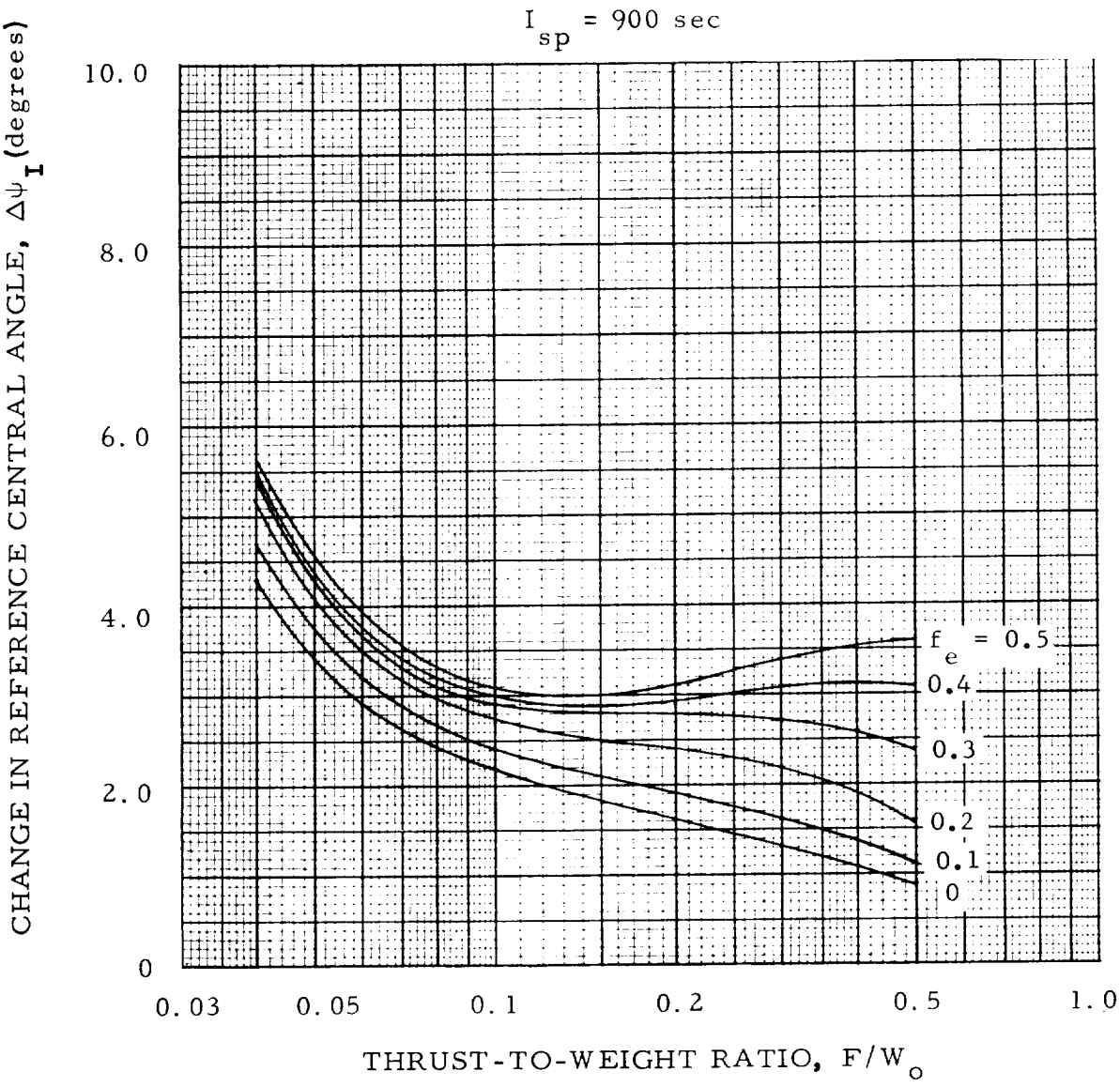

FIGURE 14b. CHANGE IN REFERENCE CENTRAL ANGLE AT INJECTION FOR NON-REFERENCE SPECIFIC IMPULSES

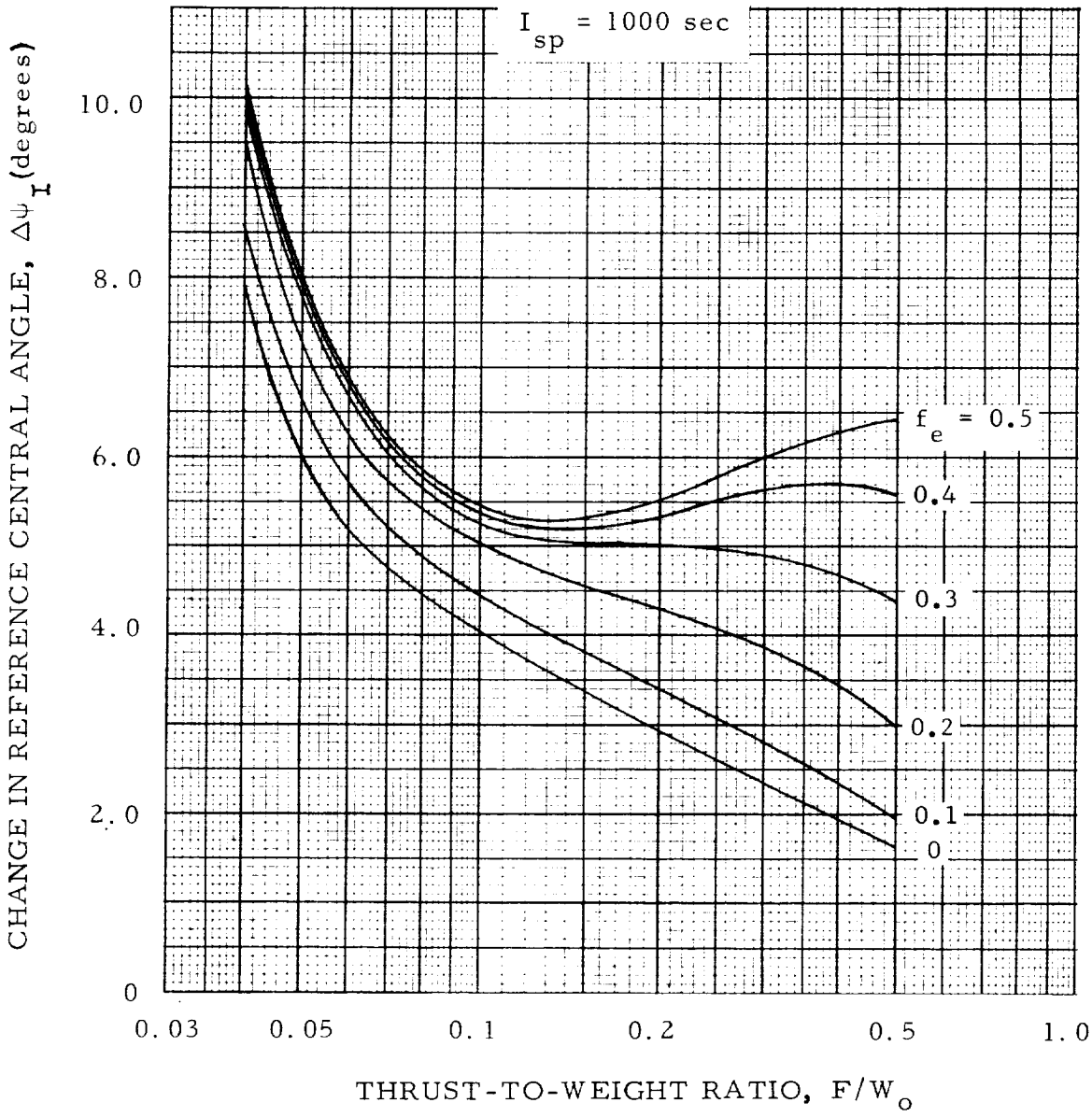

FIGURE 14c. CHANGE IN REFERENCE CENTRAL ANGLE AT INJECTION FOR NON-REFERENCE SPECIFIC IMPULSES

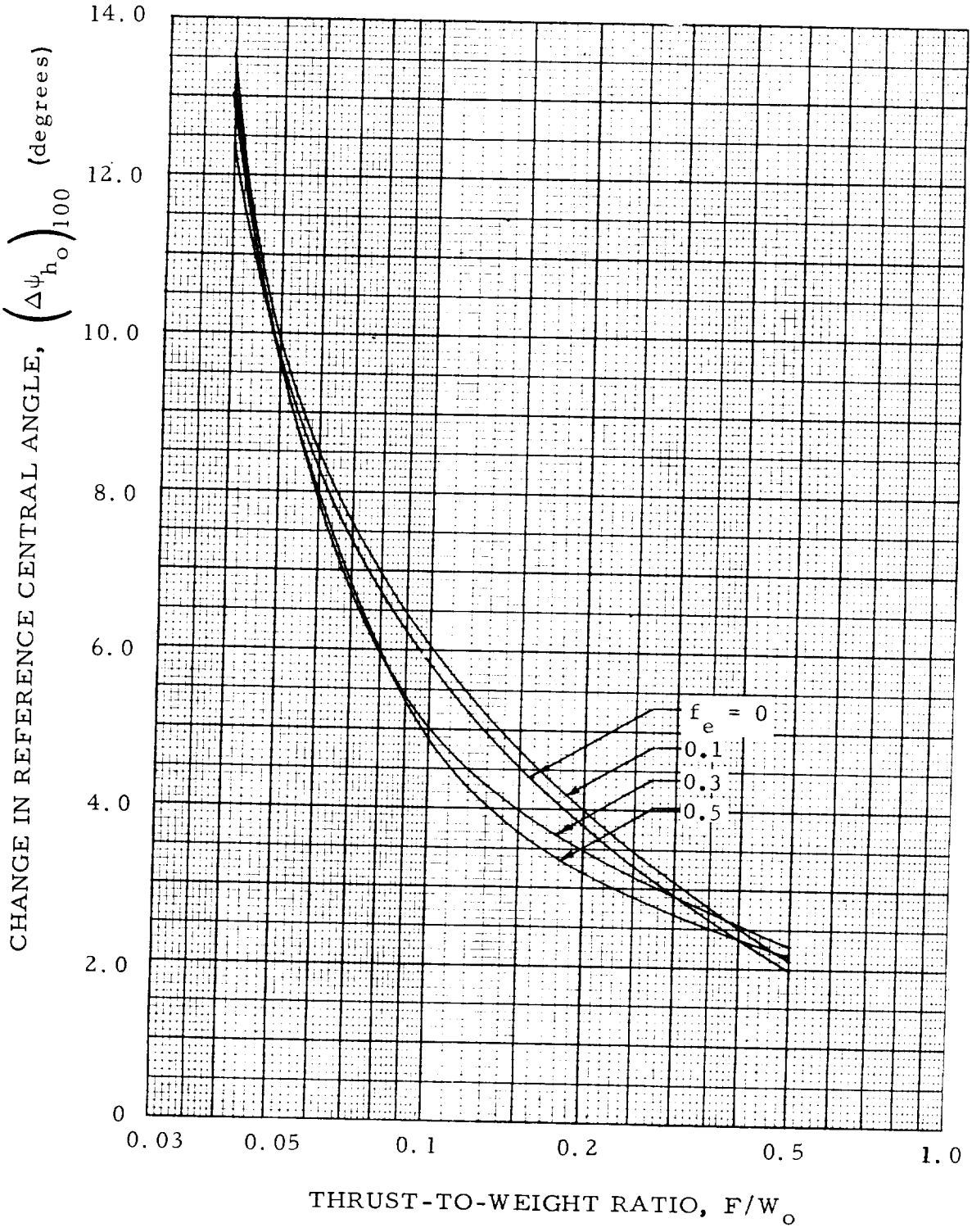

FIGURE 15. CHANGE IN REFERENCE CENTRAL ANGLE AT INJECTION FOR INCREMENTAL ALTITUDE DECREASE OF 100 N. M.

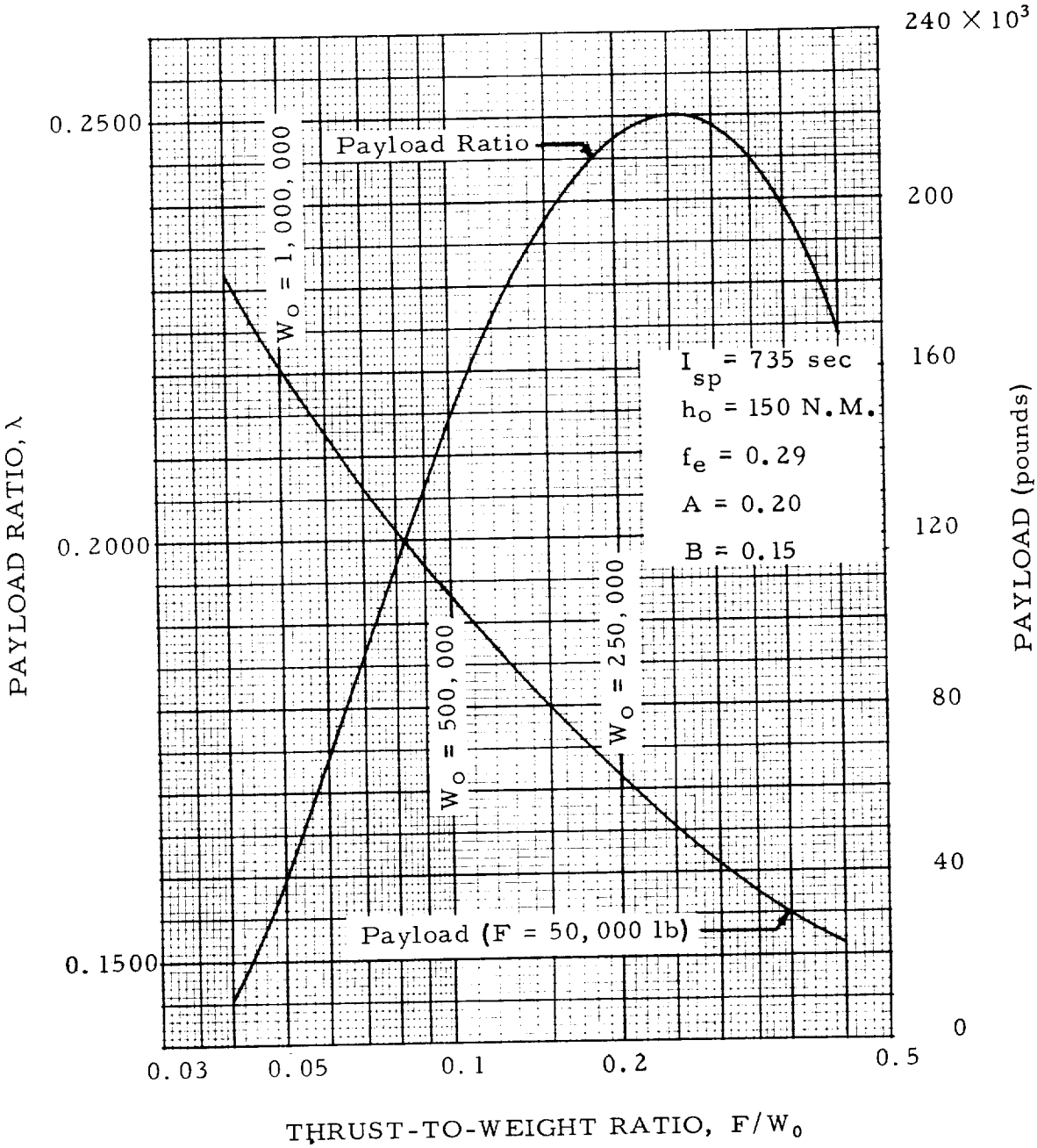

FIGURE 16. PAYLOAD RATIO AND FIXED THRUST PAYLOAD FOR DATA OF EXAMPLE 1

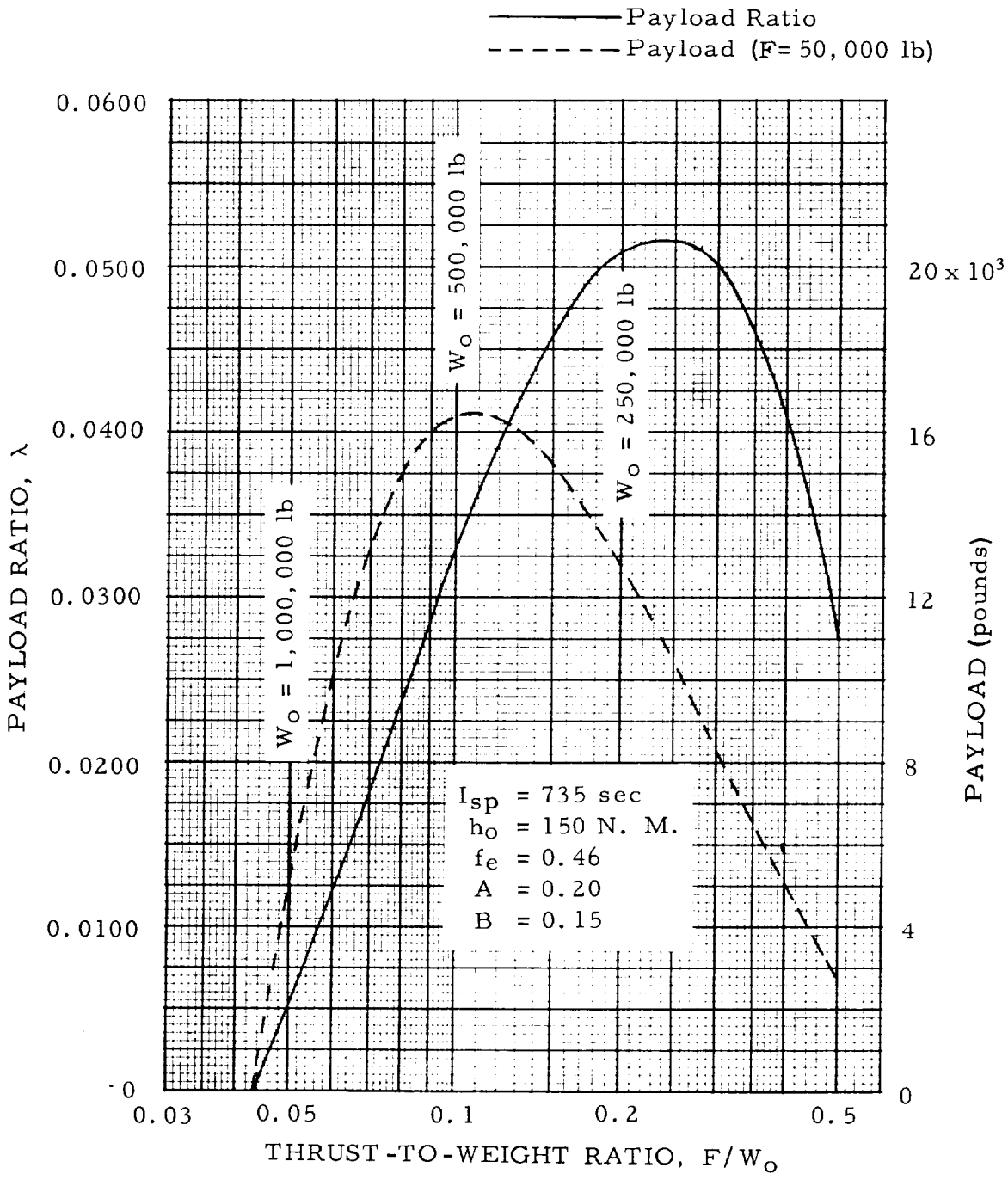

FIGURE 17. PAYLOAD RATIO AND FIXED THRUST PAYLOAD FOR VEHICLE OF EXAMPLE 1 AND HIGH HYPERBOLIC EXCESS SPEED

Table 1. Data Assumed for Numerical Examples

Example Number →	1	2	3	4	5
I_{sp} (sec)	735	885	980	750	940
h_o (N. M.)	150	375	250	100	525
F/W_o	0. 20	0. 10	0. 40	0. 30	0. 23
f_e	0. 29	0. 35	0. 43	0. 18	0. 42
A	0. 20	0. 08	0. 09	0. 05	0. 20
B	0. 15	0. 07	0. 15	0. 12	0. 15
C	0	0. 01	0. 02	0. 03	0. 01

Example Number	1			2			3			4			5				
Variable	Pred.	Actual	Error	Pred.	Actual	Error	Pred.	Actual	Error	Pred.	Actual	Error	Pred.	Actual	Error	Maximum Error*	Average Error*
λ	0.2491	0.2478	0.5%	0.2754	0.2749	0.2%	0.2074	0.2113	0.2%	0.4295	0.4293	0%	0.1817	0.1847	1.6%	0.5%	0.2%
ζ	0.6207	0.6193	0.2%	0.6614	0.6609	0.1%	0.6380	0.6371	0.1%	0.4695	0.4694	0%	0.6603	0.6602	0%	0.4%	0.2%
ΔV_{id} (m/sec)	6993.9	6971.1	0.3%	9410.3	9397.4	0.1%	9780.5	9755.7	0.3%	4669.3	4667.1	0%	9966.0	9964.1	0%	0.4%	0.2%
t_b (sec)	2281.1	2276.0	0.2%	5853.4	5848.6	0.1%	1563.1	1561.0	0.1%	1173.8	1173.4	0%	2698.6	2698.3	0%	0.4%	0.2%
ψ (sec)	133.8	133.2	0.5%	194.7	196.4	0.7%	103.5	103.8	0.3%	86.7	86.8	0.1%	127.5	130.8	2.5%	0.7%	0.4%
θ (deg)	40.8	40.5	0.7%	24.1	23.7	1.7%	39.0	39.3	0.8%	60.6	60.7	0.2%	30.6	30.3	0.1%	1.7%	0.8%
h_b (N.M.)	4491	4330	3.7%	14105	14905	5.4%	3345	3731	10.3%	1258	1271	1.1%	6809	7426	8.3%	10.3%	5.5%

*Does not include Example 5 since initial altitude is outside the range considered (see table 1).

TABLE 2. COMPARISON OF EXACT AND PREDICTED PERFORMANCE PARAMETERS

REFERENCES

1. Fellenz, Dietrich W. and Harris, Ronald J., Influence of Weight Parameters on the Propulsion Requirements of Orbit-Launched Vehicles. NASA TN D-1525, November, 1962.

2. Ruppe, H. O., Interplanetary Flight. Handbook of Astronautical Engineering, Section 9. 23, Edited by H. H. Koelle, McGraw Hill, 1961.

3. Ehrike, K. A., Principles of Guided Missile Design - Space Flight. Vol. I, Edited by Grayson Merrill, D. Van Nostrand Company, Inc., 1960.

4. Breakwell, J. V., Gillespie, R. W. and Ross, S., Researches in Interplanetary Transfer. ARS Preprint 954-59, presented at Fourteenth Annual Meeting, Washington, D. C., November 1959.

5. A Study of Interplanetary Transportation Systems. Contract NAS 8-2469, Lockheed Missiles and Space Company, June 2, 1962.

6. Moeckel, W. E., Trajectories with Constant Tangential Thrust in Central Gravitational Fields. NASA TR R-53, 1959.